American Physical Society
1963 Winter Meeting in the
West, Pasadena, California
December 19-21, 1963

X-640-63-179

THE SOLAR WIND GEOMAGNETIC FIELD BOUNDARY

BY
DAVID B. BEARD

AUGUST 1963
GODDARD SPACE FLIGHT CENTER
GREENBELT, MARYLAND

DISCLAIMER

THE SOLAR WIND GEOMAGNETIC FIELD BOUNDARY

David B. Beard*
National Aeronautics and Space Administration
Goddard Space Flight Center
Greenbelt, Maryland

ABSTRACT

The theory of the boundary of the cavity surrounding a magnetic dipole immersed in a steadily flowing stream of plasma is reviewed, and the various results compared with satellite observations of the termination of the geomagnetic field. The shape on the solar side is roughly hemispherical with some theoretical uncertainty over the poles; the shape on the antisolar side is probably raindrop shaped but depends critically on the direction and relative magnitude of the interplanetary magnetic field and possible non-adiabatic processes such as shock phenomena.

---

*On leave from University of California, Davis, for the summer as a National Academy of Sciences--National Research Council Senior Resident Research Associate (summer 1963).

INTRODUCTION

The correlation between solar flares and subsequent magnetic storms observed on the surface of the earth first led Chapman and Ferraro [1931, 1932, 1933, 1940, and Ferraro 1952] thirty years ago, to consider the interaction between the geomagnetic field and a sheet of plasma emanating from the sun. Chapman [1962, 1963] has written an exemplary review of this pioneer work and its subsequent development. It was immediately recognized that the diamagnetic behavior of the solar plasma would exclude the geomagnetic field by means of electric currents on the surface of the plasma and that the geomagnetic field would be compressed and limited to a sharply defined volume from which the solar plasma was excluded. Later Bierman [1951] pointed out that the appearance of comet tails could not be explained by solar light pressure as previously thought and instead required the constant presence of a steadily streaming solar plasma. The suggestion of a constant plasma stream emanating from the sun received valuable theoretical corroboration from Parker [1958] who suggested the term "solar wind" and has recently been conclusively demonstrated by satellite experiments [Freeman,

Van Allen, and Cahill 1963, and Neugebauer and Snyder 1962]. Ferraro [1952] and Dungey, [1958] who has contributed much further insight into the problem, in particular showed that if an electric field were present at the boundary due to charge separation resulting from the difference in momentum between the positive ions and electrons, the boundary layer would be infinitesimally thin.

A calculation of the exact shape of the boundary surface remained [illegible] of the magnetic field at the surface. That is, the calculation of the boundary shape required a knowledge of the magnetic field resulting from the electric currents in the boundary surface which in turn could not be calculated until the boundary shape was determined. Recently several independent approximate numerical calculations [Beard 1960, 1962, Midgley and Davis 1962, and Slutz 1962] have surmounted this difficulty and resulted in a boundary shape which is particularly well understood on the solar side of the earth. It is in the inherent nature of the approximations that the polar regions are only roughly correct at this time. The boundary shape on the antisolar side of the earth depends critically on the theoretically not as yet well-understood effect of an interplanetary magnetic field and the random (thermal) energy of the particles in the solar stream. Thus the antisolar shape of the boundary is only qualitatively understood at the present time.

THE PHYSICS OF THE BOUNDARY LAYER

THE THICKNESS OF THE BOUNDARY LAYER

Fig. 1 illustrates representative naive trajectories of charged particles incident perpendicularly on a magnetic field confined within a cylinder whose axis is parallel to the magnetic field. The positive ions will penetrate more deeply than the electrons into the boundary layer because of their greater momentum. The resulting charge separation will create an electric field perpendicular to the surface and directed outwards. The electric field exists only in the boundary layer and creates a total potential difference equal to the kinetic energy of the stream of positive ions causing it, divided by the electric charge on the ions. As a result the incident ions are decelerated in the electric field and reflected from the innermost boundary towards the outer layer of negative charge. That is, the ions are reflected primarily by the electric field. On the other hand, the electrons are accelerated by the electric field to a maximum kinetic energy equal to the original kinetic energy of the ions in the stream and are deflected by the magnetic field in the boundary. The velocity of the electrons parallel to the boundary layer greatly exceeds that of the ions, and the electrical current in the boundary is generated by the flow of electrons. Grad [1961], Paskievici, Sestero, and Weitzner [1962], and MacMahon have examined the orbits of charges in the boundary layer in detail, but it is enough for our purposes to adapt Dungey's [1958] and Rosenbluth's [1957] calculation of the magnetic field in the

boundary [Beard 1960] and to show that it decreases in an infinitesimal distance. The actual trajectories as computed by MacMahon (private communication) are illustrated in Fig. 2.

Let the z axis be antiparallel to the magnetic field interior and parallel to the surface and the y axis of a right handed coordinate system be in the plane of the surface, then the particle equations of motion will be

$$m\ddot{x} = eE(x) + (e/c)B\dot{y} \tag{1}$$

$$m\ddot{y} = -(e/c)B\dot{x} \tag{2}$$

Noting that $\int \frac{dx}{dt} dt = \int dx$, integrating Eq. 2, and substituting the result into Eq. 1, we obtain

$$v_y = v_{oy} - (e/mc) \int_{-\infty}^{x} B dx' \tag{3}$$

$$\dot{x}\ddot{x} = \frac{e}{m} E(x)\dot{x} + \frac{e}{mc} B v_{oy} \dot{x} - \frac{e^2}{mc^2} \frac{1}{2} \frac{\partial}{\partial x} \left[\int_{-\infty}^{x} B dx' \right]^2 \dot{x}$$

$$v_x^2 = v_{ox}^2 + 2(e/m) \int_{-\infty}^{x} [E + (v_{oy}/c)B] dx' - (e/mc)^2 \left[\int_{-\infty}^{x} B dx' \right]^2 \tag{4}$$

where v_{ox} and v_{oy} are the initial velocity components of the plasma stream at negatively infinite x.

The particle density is given by

$$N = 2N_o v_{ox}/v_x \tag{5}$$

where N_o is the field-free space particle density. Charge neutrality must occur to a high degree of approximation if the electrical potential energy of the particles is not to exceed the initial kinetic energy of the ions. Hence the x component of the ion and electron velocities must be equal. Since the initial ion and electron velocities are equal, equating Eq. 4 for the electron and ion velocities and neglecting terms of order m_e/m_i we obtain

$$\int_{-\infty}^{x} E dx' = - (v_{oy}/c) \int_{-\infty}^{x} B dx' - (e/2m_e c^2) \left[\int_{-\infty}^{x} B dx'\right]^2 \tag{6}$$

where the subscripts i and e are used for ion and electron respectively. Eq. 6 amounts to requiring the electrons to follow the ions into the boundary to prevent charge separation and yields the integral over E (the loss in potential energy of the electrons) required for the electrons' increase in kinetic energy in penetrating more deeply into the magnetic field than they would penetrate in the absence of an electric field.

Substituting Eq. 6 into Eq. 4, one obtains the x component of the ion velocity which is equal to the same component of the electron velocity

$$v_{ix}^2 = v_{ox}^2 - (e^2/m_e m_i c^2)\left[\int_{-\infty}^{x} B dx'\right]^2 \tag{7}$$

The surface current and field may be related by Maxwell's equation

$$\text{curl } B = \frac{\partial |B|}{\partial x} = 4\pi j = -4\pi (2N_o v_{ox}/v_{ix})(e/c)v_{ey} \tag{8}$$

in which the ion contribution to the current has been neglected since $v_i \ll v_e$. Substituting Eq. 4 and 7 into Eq. 8 we obtain

$$\frac{\partial B}{\partial x} = -\left[8\pi N_o e v_{ox}/c \left(v_{ox}^2 - \left\{ e^2/m_e m_i c^2\right\}\left\{\int_{-\infty}^{x} B dx'\right\}^2\right)^{\frac{1}{2}}\right]$$

$$X\left[v_{oy} - (e/m_e c)\int_{-\infty}^{x} B dx'\right] \tag{9}$$

$$\sim -8\pi N_o (e/c)\left[v_{oy} - (e/m_e c)\int_{-\infty}^{x} B dx'\right]$$

$$\frac{\partial^2 B}{\partial x^2} - \frac{8\pi N_o e^2}{m_e c^2} B \sim 0$$

$$B \sim B_o e^{x/x_o} \tag{10}$$

where $x_o = (m_e c^2/8\pi N_o e^2)^{\frac{1}{2}} = 2/\sqrt{N_o}$ km, and x is negative and measured from the deepest edge of the layer of positive charge. Eq. 9 may be solved exactly, but the extremely cumbersome result is required only for $-x \ll x_o$. The importance of the result we have obtained is that the few ions per cc in the solar plasma will cause the boundary layer to be of the order of a kilometer thick and hence of negligible thickness.

At one time it was pointed out to me by E. N. Parker that the foregoing calculation has neglected the contribution made by the high electrical conductivity along the magnetic lines of force. The magnetic lines of force in the boundary layer are grounded in the earth's ionosphere. Electrons are free to move in and out of this infinite reservoir of charge and in time will ground the boundary layer so that no electric field will exist in a steady state problem in which no change occurs in the pressure of the solar wind. In this case the protons, not the electrons, will cause the surface current because of their larger radius of curvature in the boundary layer. The thickness of the boundary layer in this case will clearly be related to the radius of the ion cyclotron orbits in the magnetic field of the boundary layer. The magnetic field is given by the integral of the current density over the depth of the boundary. If the ions moved in a constant magnetic field, the ions position measured from their point of deepest penetration is given for $0 < x < r$ by

$$x = r\,(1 - \cos\theta),\quad y = r\sin\theta$$

where r is the ion cyclotron radius and θ is the phase of their orbit measured from the point of deepest penetration. The current density is given by

$$J = N(e/c)\,v_y = N_o(e/c)\,(v/v_x)\,v_y$$

where v is the stream velocity. Taking the time derivatives of x and y we find

$$J = eN_o(v/c)(1 - x/r)/(2x/r - x^2/r^2)^{\frac{1}{2}}$$

For a plane current distribution for $0 < x < r$:

$$B = \frac{2\pi}{c}\int_o^x Jdx' - \frac{2\pi}{c}\int_x^r Jdx' = 4\pi eN_o(v/c^2)\left[(2x/r - x^2/r^2)^{\frac{1}{2}} - \frac{1}{2}\right] \qquad (11)$$

This crude estimate yields the result that 80% of the magnetic field due to the surface current is experienced within half the ion cyclotron radius from the innermost edge of the boundary. Since $r < 40$ km for any reasonable values of the solar wind, the surface layer is of the order of 10 km thick, again infinitesimally thin compared with the radius of curvature of the surface.

PRESSURE BALANCE AT THE BOUNDARY

In either case of boundary electric field or no boundary electric field, it is easy to show that specular reflection must occur for the particles incident on a steady state smooth surface. If the electric field perpendicular to the surface and the magnetic field tangential to the surface are symmetric about a plane perpendicular to the particle's orbit at the point of deepest penetration, then the exit path of the particle from the surface must be the mirror image of its incident path. Thus the angle of incidence of the stream velocity vector with the normal vector to the surface is equal to the angle of reflection of the particle emerging from the surface boundary. The total momentum change of a particle

reflected from the surface is thus equal to 2 mv cos ψ where mv is the particle's momentum and ψ is the angle of incidence. (If the surface is moving, $\underset{\sim}{v}$ is the relative velocity of the particle and surface.) The number of particles striking the surface per second per unit area is Nv cos ψ where N is the density of particles in the solar wind. Therefore the total pressure of the particles perpendicular to the surface is given by

$$p = 2N\, mv^2 \cos^2\psi \tag{12}$$

where m is the mass of the ions since the pressure of the electrons is negligible.

A conducting fluid moving in electric and magnetic fields will experience forces expressed by familiar magnetohydrodynamic equations [Spitzer, 1956]

$$\text{grad } p = \underset{\sim}{j} \times \underset{\sim}{B}/c \tag{13}$$

where $\underset{\sim}{j}$ is the electrical current density in the fluid. Eq. 13 may be rewritten for the magnetosphere boundary in which $\underset{\sim}{j}$, $\underset{\sim}{B}$, and grad p are mutually perpendicular as

$$\underset{\sim}{j}/c = \underset{\sim}{B} \times \text{grad } p/B^2 \tag{13'}$$

Maxwell's equation,

$$\text{curl } \underset{\sim}{B} = 4\pi\, \underset{\sim}{j}/c \tag{14}$$

may be substituted into Eq. 13 to obtain

$$\text{grad } p = (1/4\pi)(\underset{\sim}{B} \cdot \text{grad})\underset{\sim}{B} - (1/8\pi)\, \text{grad } B^2$$

The change in the magnetic field in the direction of the magnetic field is negligible compared to the change in the field perpendicular to the boundary in the direction of $\underset{\sim}{p}$. Therefore the first term may be neglected

and the equation integrated to yield the well-known diamagnetic approximation in magnetohydrodynamics

$$p + B^2/8\pi = \text{constant} \tag{15}$$

Letting the constant be the free space value of the stream pressure, $p_o = 2nmv^2$, $p = 2nmv^2 \cos^2\psi$, we obtain the pressure equation relating the particle pressure outside the boundary to the magnetic pressure inside the boundary. This equation determines the surface.

$$B = \pm(8\pi p)^{\frac{1}{2}} = \pm(16\pi nmv^2)^{\frac{1}{2}} \cos\psi = \pm(8\pi p_o)^{\frac{1}{2}} \cos\psi \tag{15'}$$

Since the normal component of $\underset{\sim}{B}$ is continuous across the surface and must be zero outside the surface, the magnetic field interior and close to the surface is everywhere tangential to the surface. Therefore Eq. 15' may be rewritten as

$$|\hat{\underset{\sim}{n}}_s \times \underset{\sim}{B}| = -(8\pi p_o)^{\frac{1}{2}} \hat{\underset{\sim}{n}}_s \cdot \hat{\underset{\sim}{v}} \tag{16}$$

where $\hat{\underset{\sim}{n}}_s$ is the unit normal to the surface and $\hat{\underset{\sim}{v}}$ is the unit vector in the direction of the stream velocity. Since $\hat{\underset{\sim}{n}}_s \cdot \hat{\underset{\sim}{v}}$ must be negative everywhere on the surface in order for the outside of the surface to be exposed to the solar stream, the minus sign appears in Eq. 16.

The surface is defined by a function $F(r, \theta, \Phi) = \text{constant}$. Let the constant be zero and the function be

$$F(r, \theta, \Phi) = r - R(\theta, \Phi) = 0 \tag{17}$$

then the normal to the surface is written

$$\hat{\underset{\sim}{n}}_s = \text{grad } F/|\text{grad } F| = a\left(\hat{\underset{\sim}{r}} - \frac{1}{r}\frac{\partial R}{\partial \theta}\hat{\underset{\sim}{\theta}} - \frac{1}{r \sin\theta}\frac{\partial R}{\partial \Phi}\hat{\underset{\sim}{\Phi}}\right) \tag{18}$$

where

$$a = \left[1 + \frac{1}{r^2}\left(\frac{\partial R}{\partial \theta}\right)^2 + \frac{1}{r^2 \sin^2\theta}\left(\frac{\partial R}{\partial \Phi}\right)^2\right]^{-\frac{1}{2}}$$

In a polar coordinate system where the dipole is opposite to the direction of the polar axis and the velocity vector of the incoming stream makes an angle λ with the magnetic equatorial plane, see Fig. 3, $\hat{\underset{\sim}{v}}$ is written

$$\begin{aligned}\hat{\underset{\sim}{v}} = &- (\cos\theta \sin\lambda + \cos\Phi \sin\theta\cos\lambda)\hat{\underset{\sim}{r}} \\ &- (\cos\Phi \cos\theta \cos\lambda - \sin\theta \sin\lambda)\hat{\underset{\sim}{\theta}} \\ &+ \sin\Phi \cos\lambda \hat{\underset{\sim}{\Phi}}\end{aligned} \tag{19}$$

Therefore

$$\begin{aligned}\hat{\underset{\sim}{n}}_s \cdot \hat{\underset{\sim}{v}} = a\Big[&- \cos\Phi \sin\theta \cos\lambda - \cos\theta \sin\lambda \\ &+ (\cos\Phi \cos\theta \cos\lambda - \sin\theta \sin\lambda)\frac{1}{r}\frac{\partial R}{\partial \theta} \\ &- \sin\Phi \cos\lambda \frac{1}{r \sin\theta}\frac{\partial R}{\partial \Phi}\Big]\end{aligned} \tag{20}$$

When the wind is perpendicular to the dipole, $\lambda = 0$, and (20) assumes a simpler form

$$-\hat{\underset{\sim}{n}}_s \cdot \hat{\underset{\sim}{v}} = a\left[\cos\Phi \sin\theta - \cos\Phi \cos\theta \frac{1}{r}\frac{\partial R}{\partial \theta} + \frac{\sin\Phi}{r \sin\theta}\frac{\partial R}{\partial \Phi}\right] \tag{20'}$$

(N. B. λ is positive during summer in the Northern hemisphere and Φ is measured here from the subsolar line rather than from the "twilight" line as in Beard [1960].)

APPROXIMATE METHODS FOR CALCULATING THE SURFACE

THE METHOD OF THE SELF-CONSISTENT FIELD

Eq. 16 is incomplete in that we have no analytical expression to use for $\underset{\sim}{B}$. Hence the surface cannot be found from this equation until $\underset{\sim}{B}$ is known. Unfortunately, the magnetic field due to the surface currents cannot be computed until the surface is known. A way out of this impasse is to assume a reasonable value for the magnetic field in Eq. 16 [Beard 1960, 1962]. Calculate the surface resulting from this approximation, and use the calculated surface to compute new values of $\underset{\sim}{B}$. From these new values of $\underset{\sim}{B}$ calculate by a reiterative process better and better surfaces until a surface is obtained which yields a total magnetic field outside the surface less than or equal to the error in the numerical integration of the magnetic field inside the surface due to surface currents.

A reasonable value for the first approximation magnetic field is suggested by consideration of the thickness of the surface layer compared with the radius of curvature of the surface. The surface is very nearly a plane as far as points local to a particular surface point are concerned. If the surface were a plane, the field due to the surface currents would be equal and opposite on both sides of the surface. Since the field outside is zero, the plane surface current field would be equal and opposite to the geomagnetic field outside the surface and must therefore exactly double the tangential component of the geomagnetic field inside the surface. The geomagnetic field is given by

$$\underset{\sim}{B}_g = -\frac{M}{r^3}\left(2\cos\theta\ \hat{\underset{\sim}{r}} + \sin\theta\ \hat{\underset{\sim}{\theta}}\right) \qquad (21)$$

Ferraro [1960] has suggested that the first approximation may be improved by multiplying the tangential component of the geomagnetic field by a factor 2f rather than 2. Only the scale, not the shape, of the surface is affected by this change. Unfortunately the value of f cannot be computed except on the way to a higher order approximation. The value of f has been found to be reasonably close to 1, as expected, when the second order calculation is made.

When Eq. 18, 20, and twice 21 are substituted into Eq. 16 a first approximation surface may be computed. A solution of Eq. 16 may not exist, however, for all angles, θ and Φ, if the correct value of $\underset{\sim}{B}$ is not used. In this case, to obtain a corrected magnetic field from a previous approximation surface, the surface must be arbitrarily constructed for values of θ and Φ for which no solution exists in the previous approximation. A further approximation which enables more of the first approximation surface to be calculated than is possible using Eq. 16, is to assume that all components other than the $\hat{\underset{\sim}{\phi}}$ component of $\hat{\underset{\sim}{n}}_s \times \underset{\sim}{B}$ are zero. [Davis and Beard 1962] This approximation gives an exact expression only in the meridian and equatorial planes and on the surface of a sphere (which fortunately the sunlit surface resembles). Using this approximation we construct a unit vector $\hat{\underset{\sim}{P}}$ parallel to $\underset{\sim}{B}$ inside the surface.

$$\hat{\underset{\sim}{P}} = k(\hat{\underset{\sim}{\phi}} \times \hat{\underset{\sim}{n}}_s) = - b'\left(\frac{1}{r}\frac{dR}{d\theta}\hat{\underset{\sim}{r}} + \hat{\underset{\sim}{\theta}}\right)$$

where

$$b' = \left[1 + \frac{1}{r^2}\left(\frac{dR}{d\theta}\right)^2\right]^{-\frac{1}{2}}$$

Therefore

$$|\hat{n}_s \times \underset{\sim}{B}| \sim 2\hat{P} \cdot \underset{\sim}{B} = 2\frac{b'M}{r^3}\left(\sin\theta + \cos\theta \frac{2}{r}\frac{dR}{d\theta}\right) \tag{22}$$

In the meridian plane $\frac{dR}{d\Phi} = 0$, Eq. 22 is exact, and the equation resulting from substituting Eqs. 20' and 22 into 16 assumes a particularly simple form

$$\frac{2M}{(8\pi p_o)^{\frac{1}{2}}}\frac{1}{r^3}\left[\sin\theta + \cos\theta \frac{2}{r}\frac{dR}{d\theta}\right] = \sin\theta - \cos\theta \frac{1}{r}\frac{dR}{d\theta} \tag{23}$$

Let

$$R_o = (M^2/4\pi mnv^2)^{1/6} = (M^2/2\pi p_o)^{1/6}$$

and let r be measured in units of R_o, then Eq. 23 becomes

$$\frac{dR}{d\theta} = r \tan\theta \frac{r^3 - 1}{r^3 + 2} \tag{24}$$

whose solution is

$$r = 1 \tag{25}$$

or

$$\frac{r_o^3 - 1}{r_o^2}\frac{r^2}{r^3 - 1} = \cos\theta \tag{26}$$

where the constant r_o occurring in the integration constant is the value of r at $\theta = 0$. Eq. 26 yields a surface for which r is either zero or infinite at the equator ($\theta = 90^\circ$) and with infinite slope. Eq. 25, for a circle, yields a much more acceptable surface.

At the pole ($\theta = 0$), $\hat{n}_s \cdot \hat{v} = 0$, and the field B and current j change direction. Since B changes direction, the right hand side of Eq. 22 becomes negative and of wrong sign since it represents the absolute value of $|\hat{n}_s \times B|$. Multiplying the right hand side of Eq. 22 by - 1 and using it in Eq. 16 we obtain the equation for the meridian plane on the antisolar side:

$$\frac{dR}{d\theta} = r \tan\theta \frac{r^3 + 1}{r^3 - 2} \tag{27}$$

whose solution is

$$\frac{kr^3}{1 + r^3} = r \cos\theta \tag{28}$$

Spreiter and Briggs [1962] have made many illuminating graphs of Eqs. 25, 26, and 28.

Eq. 28 does not connect with $r = 1$ at $\theta = 0^\circ$. A surface solution does not exist in first approximation near the pole on the antisolar side. Beard [1960] attempted a different problem beyond and near the pole by treating the perpendicular component of the field. The resulting solution had the advantage of necessarily having the slope of the surface vary continuously. Spreiter and Briggs [1962] extended the antisolar solution over to the solar side until it intersected the daylight solution at $\theta = 19.1^\circ$. This procedure leads to difficulty in higher approximation, and the non-continuous slope yields an infinite magnetic field component perpendicular to the surface, but it places the null point (where $\hat{n}_s \cdot \hat{v} = 0$) on the solar side where it should be. A third procedure

may be based on a private observation of Leverett Davis that the point at infinity in the meridian plane must be at twice the height of the null point because of current conservation. Setting k = 2 in Eq. 28, let Eq. 28 represent the solution for $30^\circ < \theta < 90^\circ$ and interpolate by a simple power series for $0 < \theta < 30^\circ$ so that the solution and its derivative match at $\theta = 0^\circ$ and 30°.

$$\Phi = 180^\circ \qquad 0 < \theta < 30^\circ \qquad r = 1 + 0.00535\theta^{3/2} + 0.000222\theta^2$$

The various first approximation surfaces are illustrated in Fig. 4.

If Eqs. 20 and 22 are substituted in Eq. 16, the surface differential equations in the meridian plane for $\lambda \neq 0$ are

$$\frac{dR}{d\theta} = r\,\frac{r^3\sin(\theta + \lambda) \mp \sin\theta}{r^3\cos(\theta + \lambda) \pm 2\cos\theta}, \qquad \Phi = 0^\circ \qquad (24', 27')$$

$$\frac{dR}{d\theta} = r\,\frac{r^3\sin(\theta - \lambda) \pm \sin\theta}{r^3\cos(\theta - \lambda) \mp 2\cos\theta}, \qquad \Phi = 180^\circ \qquad (24'', 27'')$$

Where the upper signs are to be used on the solar side of the null point and the lower signs on the antisolar side. Chapman [1963] has obtained the solutions

$$r^3\cos(\theta + \lambda) \mp \cos\theta = Kr^2 \qquad (25'26'28')$$

and similarly for 24" and 27".

Spreiter and Briggs [1962] have done a rather complete job of calculating the meridian plane first approximation solution for $\lambda \neq 0$ and these solutions are illustrated in Fig. 5.

The solution in the equatorial plane may be obtained by numerically solving Eq. 16 using Eq. 20'

$$\left(\frac{1}{r^6} - \sin^2\Phi\right)\frac{1}{r^2}\left(\frac{dR}{d\Phi}\right)^2 - 2\sin\Phi\cos\Phi\,\frac{1}{r}\frac{dR}{d\Phi} + \frac{1}{r^6} - \cos^2\Phi = 0 \qquad (29)$$

In cylindrical coordinates with the z axis parallel to the wind velocity the surface equation in the equatorial plane takes an especially simple form

$$\frac{\partial R}{\partial z} = \frac{1}{\left[\left(r^2 + z^2\right)^3 - 1\right]^{\frac{1}{2}}}$$

The solution in the equatorial plane is illustrated in Fig. 6 and tabulated in Table 1.

For regions on the surface other than the planes of summetry Eqs. 20' and 22 (or the exact expression for $\hat{n}_s \times B$) may be substituted in Eq. 16 which may be solved on a machine computer by Newton's Method (finding a value of r and its derivatives for which the equation is satisfied) as Mead [1962] has done or the resulting differential equation in Φ may be solved by a series expansion in powers of Φ on the solar side. [Beard 1960] The series expansion method requires successively computing a surface assuming $\frac{dR}{d\theta} = 0$, then using values of $\frac{dR}{d\theta}$ from the first computed surface to deduce a second surface and so on until insignificant changes occur between successively computed surfaces. Using the approximation (22) coefficients are obtained [Beard 1960] as a function of θ for the series expansion in Φ

$$r = 1 + \alpha\Phi^2 + \beta\Phi^4 \tag{30}$$

where Φ is expressed in radians. The coefficients are listed in table 2 and the surface is illustrated topographically in Fig. 6.

Having obtained a first order approximation surface one is now able to integrate over the surface and obtain the correction to the magnetic field due to the curvature of the surface which was assumed to be a plane in first order. The current density on the surface is given by Eq. 13', where it will be remembered that $\hat{n}_s$ is in the direction of grad p, and by Eq. 16 the current density magnitude is proportional to $\hat{n}_s \cdot \hat{v}$. We are then able to numerically compute the magnetic field due to the surface

currents by Laplace's equation

$$\underset{\sim}{B} = \int \frac{\underset{\sim}{J} \times \hat{\underset{\sim}{r}}}{cr^2} ds \tag{31}$$

where r is the vector from the point B is evaluated at to the infinitesimal surface element ds. This integral, which is computed for a spot on the surface, has a surface singularity where r = 0. Since the surface is infinitesimally thin, it matters how the singularity is treated. The result of the integration depends on whether we are on the outside, the inside, or at the center of the surface at the singularity (three points essentially coincident). Since we want only the correction to our first order approximation the center point is chosen at the singularity, the total field being had by again adding the planor field. The intensity of the current in terms of M and R_o^3 is determined by setting the planor magnetic field at the subsolar point, $2\pi J_o/c$, equal to the geomagnetic field at that point, M/R_o^3.

Eq. 16 now becomes

$$\left| \hat{\underset{\sim}{n}}_s \times (\underset{\sim}{B}_g + \underset{\sim}{B}_{p\ell} + \underset{\sim}{B}_{sc}) \right| = - (8\pi p_o)^{\frac{1}{2}} \hat{\underset{\sim}{n}}_s \cdot \hat{\underset{\sim}{v}}$$

where $\underset{\sim}{B}_{p\ell}$ is the planor field and $\underset{\sim}{B}_{sc}$ is the surface correction field. $\underset{\sim}{B}_{p\ell}$ is necessarily perpendicular to $\hat{\underset{\sim}{n}}_s$ and equal to $\frac{1}{2}(8\pi p_o)^{\frac{1}{2}} \hat{\underset{\sim}{n}}_s \cdot \hat{\underset{\sim}{v}}$ in magnitude because of the definition of J_o and R_o. Therefore

$$\left| \hat{\underset{\sim}{n}}_s \times (\underset{\sim}{B}_g + \underset{\sim}{B}_{sc}) \right| = - (2\pi p_o)^{\frac{1}{2}} \hat{\underset{\sim}{n}}_s \cdot \hat{\underset{\sim}{v}} \tag{32}$$

A more rigorous derivation of Eq. 32 is to note that $\underset{\sim}{B}_{pl,o}$ outside the surface is equal but opposite to $\underset{\sim}{B}_{pl}$ inside the surface and that the total $\underset{\sim}{B}$ outside the surface is zero. Thus, using the value of B_{pl} inside the surface, $\underset{\sim}{B}$ outside the surface is

$$\underset{\sim}{B}_T = - \underset{\sim}{B}_{pl} + \underset{\sim}{B}_g + \underset{\sim}{B}_{sc} = 0$$

and Eq. 32 follows.

Letting subscripts r and θ refer to r and θ components, the meridian plane equation, Eq. 23, becomes for r in units of R_o [Beard 1962, Beard & Jenkins 1962a]

$$\frac{1}{r^3}\left[\sin\theta + \cos\theta \frac{2}{r}\frac{\partial R}{\partial\theta}\right] + B_{sc\theta} + B_{scr}\frac{1}{r}\frac{\partial R}{\partial\theta}$$

$$- \sin\theta + \cos\theta \frac{1}{r}\frac{\partial R}{\partial\theta} = 0$$

$$\frac{dR}{d\theta} = r\tan\theta \frac{r^3[1 + B_{sc\theta}/\sin\theta] - 1}{r^3[1 - B_{scr}/\cos\theta] + 2} \tag{33}$$

The definition of R_o remains the same but the altitude of the subsolar point, which is found from equating the numerator in 33 to zero, becomes

$$r_{90} = (1 + B_{sc\theta})^{-1/3} \tag{34}$$

The result of the higher order approximations is to raise the subsolar point imperceptibly and to lower the neutral point where $\hat{\underset{\sim}{n}}_s \cdot \hat{\underset{\sim}{v}} = 0$. The neutral point is moved forward on the order of 20° from the pole. This is very close to the value Spreiter and Briggs obtained by arbitrarily extending the antisolar solution to the solar side.

The equation of a straight line parallel to the solar wind stream velocity is

$$r = a \sec\theta$$

whose derivative is

$$\frac{dr}{d\theta} = r \tan\theta$$

Referring back to Eq. 33 we find that the null point occurs at the angle where the coefficient of r tanθ in Eq. 33 is 1 [Beard 1962, Beard & Jenkins 1962a], that is, where

$$B_{sc\theta} \csc\theta + B_{scr} \sec\theta = 3/r^3$$

At the null point the planor field and the current change sign so that the equation in the meridian plane for θ less than the null point becomes

$$\frac{dr}{d\theta} = r \tan\theta \frac{r^3[B_{sc\theta} \csc\theta - 1] - 1}{r^3[- B_{scr} \sec\theta - 1] + 2} \qquad (35)$$

Another way of seeing Eq. 35 is to note that the total $\underset{\sim}{B}$ in Eq. 32 reverses sign at the point where $\hat{\underset{\sim}{n}}_s \cdot \hat{\underset{\sim}{v}} = 0$, and therefore we again multiply the right hand side of 22 by - 1 as we did in obtaining Eq. 27.

At the pole $B_{g\theta}$ and the unit vector $\hat{\underset{\sim}{\theta}}$ both change direction together so that $B_{g\theta}$ maintains the same sign; all radial components and the unit vector $\hat{\underset{\sim}{r}}$ maintain the same direction; the component of $\underset{\sim}{B}_{sc}$ in the new direction of $\hat{\underset{\sim}{\theta}}$, however, does change sign. Therefore, for $\phi = 180^\circ$, Eq. 35 is replaced by

$$\frac{dr}{d\theta} = r \tan\theta \frac{r^3[B_{sc\theta} \csc\theta + 1] + 1}{r^3[B_{scr} \sec\theta + 1] - 2} \qquad (36)$$

While the equatorial regions are imperceptibly altered in higher order approximation, the polar region is significantly altered. This should be expected, for the approximation of ignoring all but local surface currents in the surface should be expected to be poor where the local surface current is zero or where the radius of the surface curvature becomes small. Midgley and Davis [1962] show, as described below, that for an isotropic plasma the polar region is only poorly described in first approximation by this method. It is only in second approximation that anything nearly as good as their results is obtained. On the other hand a two dimensional solar wind problem appears more amenable to this approximation, perhaps because the surface current is zero in the polar region where the surface curvature is greatest. Dungey, [1961], Hurley, [1961], and Zhigulev and Romishevskii [1959] have solved this problem exactly and their result is compared with the first approximation solution in Fig. 7.

The self-consistent field method is presently being used to compute the surface by means of a high-speed computer [Mead 1962]. No high-speed computer results for the entire surface have yet been published using this method.

THE MULTIPOLE FIELD EXPANSION OF MIDGLEY AND DAVIS

Midgley and Davis [1962] have worked with the boundary condition that the magnetic field in the plasma region must be identically zero. In treating the case of a uniform plasma pressure surrounding a magnetic dipole they represented the surface by a polynomial expansion

in even powers of latitude angle α.

$$\rho = C\left[1 - \sum_{s=1}^{N} c_s \alpha^{2s}\right] \tag{37}$$

The coefficients were then determined by requiring the multipole moments of the magnetic field resulting from such a surface to vanish in all lower orders higher than the dipole moment. The vector potential at a point $\underset{\sim}{r}_2$ outside the surface is given by an integral over the surface current

$$\underset{\sim}{A}(\underset{\sim}{r}_2) = \int \frac{\underset{\sim}{J}(\underset{\sim}{r})ds}{|\underset{\sim}{r}_2 - \underset{\sim}{r}|} \tag{38}$$

A may be expanded in Legendre polynomials which after integration become

$$\underset{\sim}{A}(\underset{\sim}{r}_2) = \underset{\sim}{\hat{\phi}} \sum_{n=1}^{\infty} (2\pi\rho)^{\frac{1}{2}} \frac{{R_o'}^{n+2}}{n(n+1)} \frac{P_n'(\sin\alpha_2)}{r_2^{n+1}} I_n \tag{39}$$

where

$$({R_o'})^3 = M(8\pi\rho_o)^{-\frac{1}{2}}$$

and

$$I_n = \int_{-\pi/2}^{\pi/2} \rho^{n+1}\left[\rho^2 + \left(\frac{d\rho}{d\alpha}\right)^2\right]^{\frac{1}{2}} P_n'(\sin\alpha)\cos\alpha \, d\alpha \tag{40}$$

Only odd numbered n are permitted from symmetry considerations. The I_n are numerically computed, and the c_s are adjusted so that all I_n up to n = 15 are zero except I_1, the dipole term. The vector potential of a dipole is $M({R_o'})^{-2} P_1(\sin\alpha_2)$ and therefore in order for the surface current field to cancel the geomagnetic dipole at all $r_2 > \rho$, $I_1 = 4$

and thus C is determined. The coefficients in Eq. 36 are listed in Table 3, and the result is illustrated in Fig. 8.

Midgley and Davis thus obtained an exceptionally good approximate solution to the particular problem of a dipole immersed in a plasma exerting uniform pressure. They tested their solution along with the first approximation to the self-consistent field method also illustrated in Fig. 8 by computing the ratio of the net field from the surface to the dipole field along the equator and the polar axis which are presented in Table 4. As can be seen from the table their solution is a significant improvement on the first approximation to the self-consistent field method. This problem, however, seems to be an especially tough test for the first approximation to the self-consistent field method in that the surface currents at the poles are very large (where the radius of curvature is very small).

The extension of the multipole expansion method of Midgley and Davis to the solar wind problem is very much more complicated not only because of requiring the vector potential to be expanded in associated spherical harmonics rather than Legendre polynomials but because the surface current is not constant in this problem. By using a generalized Newton's method a surface has been obtained by them for which the lower undesired moments were made zero. Their results which will appear in the Journal of Geophysical Research are illustrated in Fig. 9 and 10. The magnetic ratios outside the surface are very much inferior (that is, larger) to the simpler problem they solved, being typically 1-10%.

THE FREE SURFACE SOLUTION OF SLUTZ

Slutz [1962] attacked the uniform plasma pressure problem at the same time as Midgley and Davis by a different technique. He used a method developed for hydrodynamic problems by Treffitz [~~1934~~ 1916] in finding a surface free to move in seeking equilibrium between pressures on its two sides. He described the magnetic field interior to the surface by a scalar potential

$$\underset{\sim}{B} = - \text{grad } \psi \tag{41}$$

If Eq. 41 is integrated along a meridian line and the magnetic pressure interior to the surface is equated to the particle pressure outside, the result is

$$\psi = \int (8\pi p_o)^{\frac{1}{2}} d\zeta = (8\pi p_o)^{\frac{1}{2}} \zeta \tag{42}$$

since $\underset{\sim}{B}$ is constant and tangential to the surface. Using Green's Theorem for the potential at any interior point

$$\psi = \frac{M \cos\theta}{r^2} + \frac{1}{4\pi} \int_s \left[\frac{1}{r} \frac{\partial \psi}{\partial n}\bigg|_s - \psi\bigg|_s \frac{\partial}{\partial n}\left(\frac{1}{r}\right)\right] ds \tag{43}$$

where the first term is the dipole source term inside the surface, r is the distance from t to the surface point s, and n is in the outward normal direction to the surface. Since $\underset{\sim}{B}$ is tangential to the surface the first term in the integrand is zero, and by definition of the solid angle

$$\frac{\partial}{\partial n}\left(\frac{1}{r}\right) ds = - d\Omega$$

A cusp appears over the magnetic pole and this created a difficulty in integrating Eq. 43 as t is caused to approach the surface which was surmounted in the following way. Surround t with a sphere of radius ϵ (which approaches zero in the limit). Separate the integral into that part of the surface outside the sphere S' and that part of the surface S'' inside the sphere. As t approaches infinitesimally close to the surface and $\epsilon \to 0$, ψ may be taken outside the S'' integral as it is constant in this infinitesimal region. Therefore

$$\psi = \frac{M \cos\theta}{r^2} + \frac{1}{4\pi} \int_{S'} \psi d\Omega + \frac{1}{4\pi} \psi \int_{S''} d\Omega$$

$$= \frac{M \cos\theta}{r^2} + \frac{1}{4\pi} \int_{S'} \psi d\Omega + \frac{1}{4\pi} \psi \left[4\pi - \int_{S'} d\Omega \right]$$

We finally obtain

$$\frac{M \cos\theta}{r^2} + \frac{1}{4\pi} \int_{S'} \psi d\Omega - \frac{1}{4\pi} \psi \int_{S'} d\Omega = 0 \qquad (44)$$

If all distances are put in units of $R_o' = (M/\sqrt{8\pi p_o})^{-1/3}$ Eq. 41 and 44 become

$$\frac{\cos\theta}{r^2} + \frac{1}{4\pi} \int_{S'} \psi d\Omega - \frac{1}{4\pi} \psi \int_{S'} d\Omega = 0 \qquad (45)$$

$$\psi = \zeta \qquad (46)$$

The surface was divided into areas subtending equal arcs at the origin and Eqs. 45 and 46 solved by averaging the potential over these areas. If an arbitrary surface shape is assumed Eq. 46 will yield the potential at points along the meridian which may then be substituted into Eq. 45 as a test of how good a surface shape was assumed. The process was made to converge to a satisfactory surface by a steepest descent method in that the changes in Eq. 45 were studied as the assumed surface points were varied. A surface was obtained which differed from Midgley and Davis' solution by as little as 1% at the pole and only 3% at the equator. Slutz has also applied his method to the solar wind problem but it was necessary for him to limit the surface on the anti-solar side by adding a small uniform plasma pressure. His present result, which is less accurate than his uniform plasma pressure result, is illustrated in Fig. 11.

THE SCALE OF THE BOUNDARY

All of the theoretical determinations of the boundary concern the shape which is independent of the relative magnitudes of particle pressure and dipole moment. The size of the magnetosphere is all in terms of $R_o = (2M/\sqrt{8\pi p_o})^{1/3}$. For the plasma values measured by Mariner II [Neugebauer and Snyder 1962] $N \sim 4$ protons/cc, $v \sim 6.10^7$ cms/sec and $M = 8.06 \cdot 10^{25}$ emu, R_o is 10 earth radii. Variations in the solar wind, however, will cause the surface to increase to twelve earth radii or instead decrease to eight earth radii during a mild magnetic storm

in which the solar wind pressure will double [Cahill 1962]. The surface radius at the subsolar point will decrease to five earth radii for an exceptional storm in which the particle pressure rises an order of magnitude. As suggested initially by Chapman and Ferraro [1931], commented on by Midgley and Davis [1962], and calculated by Beard and Jenkins [1962b] in estimating the magnetic effects of magnetospheric currents, such changes in scale of the magnetosphere would result in observed sudden commencement enhancement of the surface geomagnetic field.

Slutz [1962] and others have drawn attention to the increase in scale that would be produced by ring currents of trapped radiation belts. This effect has been calculated using a rough model by Spreiter and Alksne [1962] who show that reasonable ring currents enhancement, which would occur during a magnetic storm, could increase the scale a few earth radii.

The Explorer 10, 12, and 14 determinations of the geomagnetic field [Heppner, Ness, Scearce and Spillman 1963, Cahill and Amazeen 1963] and trapped radiation [Bonetti et al., 1963, Freeman et al., 1963, and Frank, Van Allen, and Macagno 1963] are the best observations of the magnitude of the pressure of the solar wind attainable. Cahill and others observed the boundary to fluctuate around 10 earth radii from 8 to 12 earth radii near the subsolar point where the boundary was recognized as a sudden change in direction and usually decrease in magnitude of the observed magnetic field. Heppner and others observed a similar

change at 22 earth radii and about 40° from the antisolar line which is the calculated position of the boundary surface when the subsolar radius is 10 earth radii. They also observed occasional regions of fairly constant magnetic field at greater distances which might be caused by shock disturbances discussed in the following but are more apt to be caused by clumps of compressed interplanetary magnetic field. The trapped particle flux observed on Explorer XII dropped abruptly to zero within sixty km at the same position as Cahill observed abrupt changes in the magnetic field.

THE EFFECT OF THE INTERPLANETARY MAGNETIC FIELD

The previous conditions of a zero temperature wind incident on the geomagnetic field will create an infinite cylindrical hollow on the downstream side; but these conditions are unrealistic. A finite temperature or, in particular, an interplanetary magnetic field will severely modify this picture on the downstream side of the earth and will cause the hollow to be closed there at a finite distance from the earth.

The Pioneer and Mariner satellites have established the existence of an interplanetary magnetic field of approximately 5γ during quiet conditions [Coleman, Davis and Sonett 1960, Sonett, Judge, Sims and Kelso 1960, Neugebauer and Snyder 1962]. Zhigulev [1959], Dessler [1962], Kellogg [1962], Gold [1959], Axford [1962] and Spreiter and Jones [1963] have suggested that the interplanetary magnetic field could create conditions for a shock wave beyond the outer boundary of

the geomagnetic field. The evidence for such a shock structure is very tentative at the present time. Cahill and Amazeen [1963] in particular, have obtained magnetic records on Explorer 12 illustrated in Fig. 12. As can be seen in the figure the magnetic field becomes very irregular beyond the magnetosphere and changes abruptly in average direction. Whether the fluctuations are evidence of shock structure or result from compressed observed inhomogeneities in the interplanetary medium cannot be ascertained. In any case there exists the observational data that the magnetic field exterior to the boundary is almost an order of magnitude greater on the average than the interplanetary value of 5γ.

Frank, Freeman, and Van Allen [1963] observed a region approximately 12,000 km thick just beyond the magnetosphere where there was an omnidirectional flux of 10^{10} electrons/cm^{2}sec having an energy between 1 and 10 kev. This corresponds to an electron density of 6-2 electrons/cc. They have suggested that this high energy electron flux is evidence of a thermalized plasma which is part of a shock structure. It could also result from clumps of plasma being energized by compression against the surface of the magnetosphere. Electrons would have the observed energy while in the charge separated boundary layer surrounding these small clumps.

The theoretical justification for believing a shock structure exists in the absence of collisions between the particles is that the radius of the cyclotron orbits of the particles in the interplanetary

field are negligible compared with the dimensions of the surface. These considerations are believed to replace those of mean free path, and that in this way particles reflected from the surface will interfere with the incident particles and thus create conditions for a shock. Conditions in a magnetized plasma, however, are quite different from those in ordinary hydrodynamics. Cyclotron motion is essentially two dimensional and more important is a well ordered motion. It is not at all clear how well the conditions for ordinary shock waves are met in a magnetized plasma.

In the absence of a well developed theory of shock structure at the magnetosphere boundary, appeal has been made to the magnetohydrodynamic collisionless shock model of Auer, Hurwitz, and Kilb [1962]. In this model an infinite sheet of magnetized plasma suddenly has an electric field (oppositely directed on the two sides of the sheet) imposed on the surface parallel to the surface but perpendicular to the magnetic field. The plasma is permitted to move only perpendicular to the boundary and currents flow only parallel to the electric field. The comparison to the magnetosphere is suggestive but indefinite. Kellogg has described the shock wave that would be formed <u>for an ordinary gas</u> in the hope that it might be some guide to the real situation. Spreiter and Jones slightly improved Kellogg's earlier description by using the actual shape of the magnetosphere as an obstacle to the solar wind, and their result is illustrated in Fig. 13.

The central fact to be kept in mind in considering the problem is that the interplanetary magnetic field and the thermal motion of the particles exert a pressure two orders of magnitude less than the pressure exerted as a result of the stream velocity. The overwhelming pressure of the wind compresses the feeble interplanetary field tight against any obstacle such as the magnetosphere. Magnetic flux will be conserved. Since the field will be limited to a maximum value found by equating magnetic and solar wind pressures, conservation of flux furnishes a means of estimating the compressed boundary layer [Beard 1963]. For example, if the field were in the direction of the wind the interplanetary field lines would be deflected smoothly and symmetrically around the magnetosphere as illustrated in Fig. 14. Conservation of magnetic flux requires that the thickness of the boundary layer, t, at a radius from the subsolar line, r, be given by

$$\pi r^2 B_i = 2\pi r t B_c$$

and thus

$$t = \frac{r}{2}\frac{B_i}{B_c} \tag{47}$$

where B_i is the interplanetary field and B_c is the compressed field.

If the interplanetary field is aligned somewhat perpendicularly to the solar wind velocity so that the field is borne along in the wind, the field would be compressed against the magnetopause as before and slip around the sides of the magnetopause with the tangential velocity of the reflected particles. In the case of a spherical

magnetosphere surface of radius R whose dipole axis is parallel to the incident trapped field, the amount of flux incident on a projected equatorial area of unit height and length parallel to the equator, y, is $B_i yV = B_i VR\sin\theta$ where θ is measured from the wind direction with the dipole taken as origin. The amount of flux leaving this volume at the edge of the magnetosphere is $B_c tV\sin\theta$ so that

$$t = (B_i/B_c)R \tag{48}$$

In either case t will be of the order of a few earth radii depending on the fraction of the maximum possible value, B_c is. (A blob of pure field will be compressed to maximum B_c, but if it contains plasma the B_c will be less). However, Eq. 48 states that the boundary layer will decrease slowly away from the subsolar point in a direction perpendicular to the field while Eq. 47 states that the boundary layer will increase from zero thickness as one moves away from the subsolar point.

The interplanetary medium is far from homogeneous. Blobs of plasma are kept intact (prevented from diffusing) by magnetic fields which are maintained by the surface currents on the plasma. As expected, the thermal pressure of the plasma as reported by Mariner II is about equal to the interplanetary magnetic field pressure. When this inhomogeneous medium is compressed against the magnetopause fluctuations of the magnetic field in magnitude and direction as a function of distance will result. Whether this is the cause of the

observed fluctuations as illustrated in Fig. 12 cannot be determined until the spatial extent of the inhomogeneities is better known but the inhomogeneities would have to be as small as of the order of an earth radius to furnish a suitable explanation. While the direction of the magnetic field would oscillate due to the surface currents on the plasma blobs, the average direction would be tangential to the magnetopause and in general entirely unrelated to the direction of the geomagnetic field. Compression of the plasma blobs and the charge separation electric fields on their surface would create energetic electrons in the compressed layer difficult to distinguish in origin from shock induced energetic electrons. One prime effect of any non-adiabatic process such as shock phenomenon will be to increase the ratio of thermal (sideways) particle pressure to magnetic pressure in the layer beyond the magnetosphere over the value of the ratio in interplanetary space. Thus non-adiabatic processes will expand the layer over that expected from free space values of particle thermal pressure to magnetic pressure.

SUMMARY

The theoretical shape of the termination of the geomagnetic field is well understood on the solar side of the earth except for a small region near the magnetic poles. This successful understanding is possible because of the overwhelming dominance of the pressure of the solar wind. On the antisolar side of the earth, however, the effect of the pressure of the solar wind is very much changed by the thermal properties of the plasma after it has passed over the solar-side surface of the magnetosphere and particularly by the presence of an inhomogeneous interplanetary magnetic field. The antisolar surface of the magnetosphere will close quite possibly in a long tear-drop shaped tail, but the exact details of this surface have yet to be found.

On the solar side three entirely different methods of approximation have been found whose results differ little between themselves except in the polar region where none of the approximations have yet yielded a precise and reliable result. The results of the approximations are illustrated in Figs. 4, 5, 6, 9, 10, and 11. The scale of the surface (about 10 ± 2 earth radii at the subsolar point) is in good agreement with satellite determinations of the energy density of the solar wind, $r_o^3 = 2M/(32\pi u)^{\frac{1}{2}}$ where M is the geomagnetic dipole moment and u is the energy density of the solar wind, $N_o \frac{1}{2} m_p v^2$.

ACKNOWLEDGMENTS

It is my pleasure to thank Dr. Gilbert Mead for a helpful critique of the manuscript and Drs. Leverett Davis, James Midgley, Gilbert Mead, Ralph Slutz, and Mr. Alan MacMahon for permission to present material taken from their unpublished work.

REFERENCES

Auer, P. L., Hurwitz, Jr., and R. W. Kilb, Large-amplitude magnetic compression of a collision-free plasma, 2, Development of a thermalized plasma, Phys. Fluids, 5, 298-316, 1962.

Axford, W. I., The interaction between the solar wind and the earth's magnetosphere, J. Geophys. Research, 67, 3791-3796, 1962.

Beard, D. B., The interaction of the terrestrial magnetic field with the solar corpuscular radiation, J. Geophys. Research, 65, 3559-3568, 1960.

Beard, D. B., The interaction of the terrestrial magnetic field with the solar corpuscular radiation, 2, Second order approximation, J. Geophys. Research, 67, 477-483, 1962.

Beard, D. B., The effect of an interplanetary magnetic field on the solar wind, to be published.

Beard, D. B., and E. B. Jenkins, Correction to the second approximation calculation of the geomagnetic field, solar wind surface, J. Geophys. Research, 67, 4895-4896, 1962a.

Beard, D. B., and E. B. Jenkins, The magnetic effects of magnetosphere currents, J. Geophys. Research, 67, 3361-3367, 1962b.

Bonetti, A., H. S. Bridge, A. J. Lazarus, B. Rossi, and F. Scherb, Explorer 10 plasma measurements, J. Geophys. Research, 68, 4017-4063, 1963.

Bierman, L., Kometenschweife und Solare Korpuskularstrahlung, Z. Astrophys., 29, 274, 1951.

Cahill, L. J., and P. G. Amazeen, The boundary of the geomagnetic field, J. Geophys. Research, 68, 1835-1843, 1963.

Chapman, S., Idealized problems of plasma dynamics relating to geomagnetic storms, Rev. Modern Physics, 32, 919-933, 1962.

Chapman, S., Solar Plasma, Geomagnetism and Aurora in Geophysics, the Earth's Environment Les Houches Lectures 1962, pp. 373-502, edited by DeWitt, Hieblot, and Lebeau, Gordon and Breach, New York, 1963.

Chapman, S., and V. C. A. Ferraro, A new theory of magnetic storms, Terrest. Magnetism and Atmospheric Elect., 36, 77-97, 171-186, 1931; 37, 147-156, 421-429, 1932; and 38, 79-96, 1933.

Chapman, S., and V. C. A. Ferraro, The theory of the first phase of a geomagnetic storm, Terrest. Magnetism and Atmospheric Elect., 45, 245-268, 1940.

Coleman, P. J., Jr., L. Davis, Jr., and C. P. Sonett, Steady component of the interplanetary magnetic field, Pioneer V, Phys. Rev. Letters, 5, 43-46, 1960.

Coleman, P. J., Jr., L. Davis, Jr., E. J. Smith, and C. P. Sonett, The mission of Mariner II: Preliminary observations. Interplanetary magnetic fields, Science, 138, 1099-1100, 1962.

Davis, L., Jr., and D. B. Beard, A correction to the approximate condition for locating the boundary between a magnetic field and a plasma, J. Geophys. Research, 67, 4505-4507, 1962.

Dessler, A. J., Further comments on stability of interface between solar wind and geomagnetic field, J. Geophys. Research, 67, 4892-4894, 1962.

Dungey, J. W., Cosmic Electrodynamics, Cambridge University Press, 132-152, 1958.

Dungey, J. W., The steady state of the Chapman-Ferraro problem in two dimensions, J. Geophys. Research, 66, 1043-1048, 1961.

Ferraro, V. C. A., On the theory of the first phase of a geomagnetic storm, J. Geophys. Research, 57, 15-49, 1952.

Ferraro, V. C. A., An approximate method of estimating the size and shape of the stationary hollow carved out in a neutral ionized stream of corpuscles impinging on the geomagnetic field, J. Geophys. Research, 65, 3951-3953, 1960.

Frank, L. A., J. A. Van Allen, and E. Macagno, Charged particle observations on the earth's outer magnetosphere, J. Geophys. Research, 68, 3543-3554, 1963.

Frank, L. A., J. W. Freeman, and J. A. Van Allen, Recent observations of electron intensities in the earth's outer magnetosphere and beyond. State Univ. of Iowa Report SUI-63-19 June 1963 (unpublished).

Freeman, J. W., J. A. Van Allen, and L. J. Cahill, Explorer 12 observations of the magnetospheric boundary and the associated solar plasma on September 13, 1961, J. Geophys. Research, 68, 2121-2130, 1963.

Gold, T., Magnetic field in the solar system, Nuovo Cimento, Suppl. [10] 13, 318-323, 1959.

Grad, H., Boundary layer between a plasma and a magnetic field, Phys. Fluids, 4, 1366-1375, 1961.

Heppner, J. P., N. F. Ness, C. S. Scearce, and T. L. Skillman, Explorer X magnetic field measurements, J. Geophys. Research, 68, 1-46, 1963.

Hurley, J., Interaction of a streaming plasma with the magnetic field of a two-dimensional dipole, Phys. Fluids, 4, 854-859, 1961.

Hurley, J., Analysis of the transition region between a uniform plasma and its confining magnetic field. II. Phys. Fluids, 6, 83-88, 1963.

Kellogg, P. J., Flow of plasma around the earth, J. Geophys. Research, 67, 3805-3811, 1962.

Mead, G. D., Numerical Solutions to the Chapman-Ferraro problem, Program of the Western national meeting Amer. Geophys. Union, Palo Alto, California, Dec. 27-29, 1962, page 459.

Midgley, J., and L. Davis, Jr., Computation of the bounding surface of a dipole field in a plasma by a moment technique, J. Geophys. Research, 67, 499-504, 1962.

Neugebauer, M., and C. W. Snyder, The mission of Mariner II: Preliminary observations. Solar plasma experiment, Science, 138, 1095-1097, 1962.

Parker, E. N., Interaction of the solar wind with the geomagnetic field, Phys. Fluids, 1, 171-187, 1958.

Paskievici, W., A. Sestero, and H. Weitzner, Courant Institute of Mathematical Sciences, New York University, Rept. NYO9193, 1962.

Rosenbluth, M. N., Dynamics of a pinched gas, in Magnetohydrodynamics, edited by R. Landshoff, Stanford University Press, Palo Alto, 57 - 66, 1957.

Slutz, R. J., The shape of the geomagnetic field boundary under uniform external pressures, J. Geophys. Research, 67, 505-513, 1962.

Spitzer, L., Physics of Fully Ionized Gases, Interscience, New York 105 pp., 1956.

Spreiter, J. R., and A. Y. Alksne, On the effect of a ring current on the terminal shape of the geomagnetic field, J. Geophys. Research, 67, 2193-2205, 1962.

Spreiter, J. R., and B. R. Briggs, Theoretical determination of the form of the boundary of the solar corpuscular stream produced by interaction with the magnetic dipole field of the earth, J. Geophys. Research, 67, 37-51, 1962.

Spreiter, J. R., and W. P. Jones, On the effect of a weak interplanetary magnetic field on the interaction between the solar wind and the geomagnetic field, J. Geophys. Research, 68, 3555-3564, 1963.

Treffitz, E., Über die Kontraktion kreisformiger Flussigkeitsstrahlen, Z. Math. U. Phys., 64, 34, 1916.

Zhigulev, V. N., and E. A. Romishevskii, Concerning the interaction of currents flowing in a conducting medium with the earth's magnetic field, Doklady Akad. Nauk SSSR, 127, 1001, 1959 translation in Soviet Physics--Doklady, 4, 859-862, 1959.

TABLE 1

r of the plasma sheath surface in units of R_o and $|r \cos\Phi|$ as a function of Φ, the longitudinal position in the equatorial plane of the earth's magnetic dipole; $90^\circ \leq \Phi \leq 180^\circ$ corresponds to the night side of the earth. $R_o = (M^2/8\pi N_o m_i v^2)^{1/6}$

Φ	0	15	30	45	60	90	120	150	180
r	1.00	1.01	1.03	1.07	1.13	1.34	1.84	3.47	∞
$\lvert r \sin\Phi \rvert$	0	0.26	0.52	0.76	0.98	1.34	1.60	1.74	1.78

TABLE 2

Values of α and β as a function of θ, the latitude angle, where α and β are the coefficients in a series expansion of r of the plasma sheath surface as a function of Φ, the longitudinal angle from the plane containing the earth's dipole and the earth-sun line; $r = 1 + \alpha\Phi^2 + \beta\Phi^4$ in units of $R_o = (M^2/8\pi N_o m_i v^2)^{1/6}$, and Φ is expressed in radians.

θ	90°	75°	60°	45°	30°	15°
α	0.104	0.102	0.096	0.086	0.068	0.031
β	0.011	0.011	0.010	0.008	0.007	0.004

TABLE 3

Coefficients in the Equation for the Surface Using the Moment Technique

$C = 1.41395$	$c_4 = -0.000200$
$c_1 = 0.120039$	$c_5 = 0.000597$
$c_2 = 0.004180$	$c_6 = -0.000326$
$c_3 = 0.001085$	$c_7 = 0.000094$

TABLE 4

Ratio of Net Field to Dipole Field X 10^5

Distance from the Surface, Fraction of Equatorial Radius	Moment Surface		Self-consistent First Approximation	
	On the Polar Axis	In the Equatorial Plane	On the Polar Axis	In the Equatorial Plane
0.04	-905	-0.4	-61078	7126
0.08	-222	+0.2	-42966	6721
0.16	-23	0.6	-27676	5997
0.32	-2.7	0.5	-15913	4844
0.64	-0.9	0.5	-7947	3324
1.28	-0.2	0.2	-3378	1817
2.56	-0.1	0.3	-1222	773
5.12	-0.0	0.5	-386	267
10.24	0.2	0.0	-110	81

FIGURE CAPTIONS

Fig. 1. Naive charged particle trajectories in the equatorial plane for particles incident from the left on a current sheath surrounding a dipole pointed into the paper (field out of paper at boundary). Solid lines trace the paths of positive ions; dashed lines trace electron paths.

Fig. 2a, b. Charged particle trajectories in a boundary layer between a plasma and a magnetic field as computed by MacMahon.

Fig. 3. Coordinate system used in self-consistent field calculations. $\underset{\sim}{M}$ is the geomagnetic dipole and $\underset{\sim}{v}$ is the solar wind stream velocity vector. The dashed vector is the projection of $\underset{\sim}{v}$ on the magnetic equatorial plane and λ is the geomagnetic latitude position of the sun.

Fig. 4. The intersection of the magnetosphere boundary with the meridain plane for $\lambda = 0$ using the self-consistent field computational method in first approximation. The solid line is for the changed polar boundary condition. The long dashed line is the continuation of the antisolar solution. The short dashed line is for a smooth fit between subsolar and antisolar solutions. All solutions presented are for a zero temperature solar plasma containing no magnetic field. A more realistic antisolar shape would be a rain-dropped tail joining these solutions near the pole and intersecting the axis at between 3-10.

Fig. 5. The intersection of the magnetosphere boundary with the meridian plane for solar wind velocities not perpendicular to the dipole

axis as calculated by Spreiter and Briggs in first approximation.

Fig. 6. Contours of the magnetosphere boundary on the solar side. View shown is looking down on the pole and the contours are shown for various polar angles. The intersection of the magnetosphere with the equatorial plane is presented for the antisolar side as well (zero temperature, no interplanetary magnetic field).

Fig. 7. Exact and approximate cavity surfaces for a line dipole in a zero temperature plasma stream. The exact surface is presented as a solid line; the first approximation of the self-consistent field method is indicated by the dashed line.

Fig. 8. First quadrant of the cross-section of the boundary between an isotropic plasma exerting uniform particle pressure and a dipole magnetic field. The solid line is for Midgley and Davis' solution using their moment method; the dashed curve is for their first approximation surface using the self-consistent field method.

Fig. 9. Pictorial view of the magnetosphere boundary as computed by Midgley and Davis using a moment technique. Earth's dipole is along y axis and the solar wind is moving in the - z direction.

Fig. 10. Cross-sections in the moon meridian (upper half of figure) and equatorial (lower half) planes for the magnetosphere boundary surfaces calculated by the first approximation to the self-consistent field and Midgley and Davis' moment technique. The solid line is the self-consistent field surface; the dashed line a "smoothed" Midgley and Davis surface; the dotted portion is Midgley and Davis' surface before "smoothing."

Fig. 11. Cross-sections in the moon meridian of the magnetosphere boundary as computed by Slutz' "free surface" method. A small constant static pressure has been added to the solar wind pressure.

Fig. 12. Explorer 12 magnetometer observations on Sept. 30 as reported by Cahill and Amazeen showing total intensity, F, and angular orientation α and ψ. The solid smooth line is the predicted intensity in the absence of a solar plasma.

Fig. 13. Traces of magnetosphere boundary and suggested ordinary gas hydrodynamic shock for a solar wind with a stream velocity of 600 km/sec, N_o = 2.5 protons/cc, B = 5 gamma and Alfven Mach number 8.71 after Spreiter and Jones [1963].

Fig. 14. Illustration of magnetic flux conservation at the surface of the magnetosphere in the equatorial plane. Light solid lines indicate magnetic lines initially filling a circular area of radius, r, compressed within a thickness, t, against the surface of the magnetosphere. Earth's dipole position is indicated by a large dot on the axis.

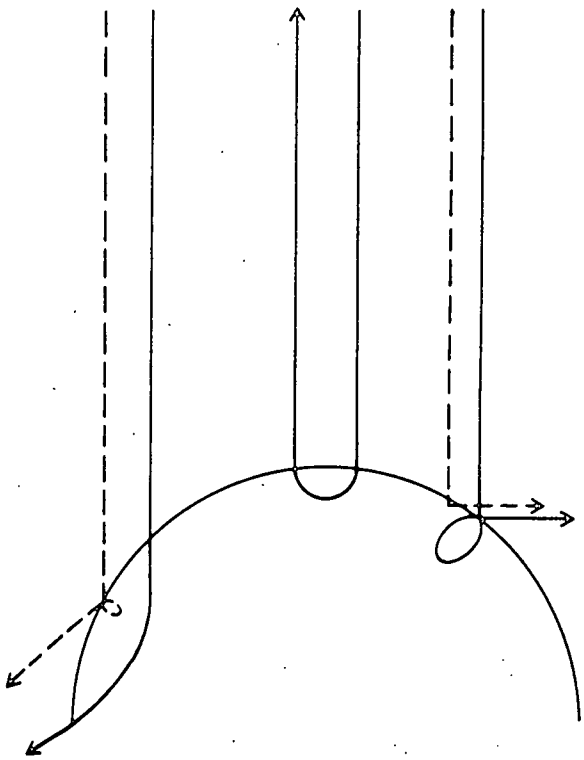

Figure 1

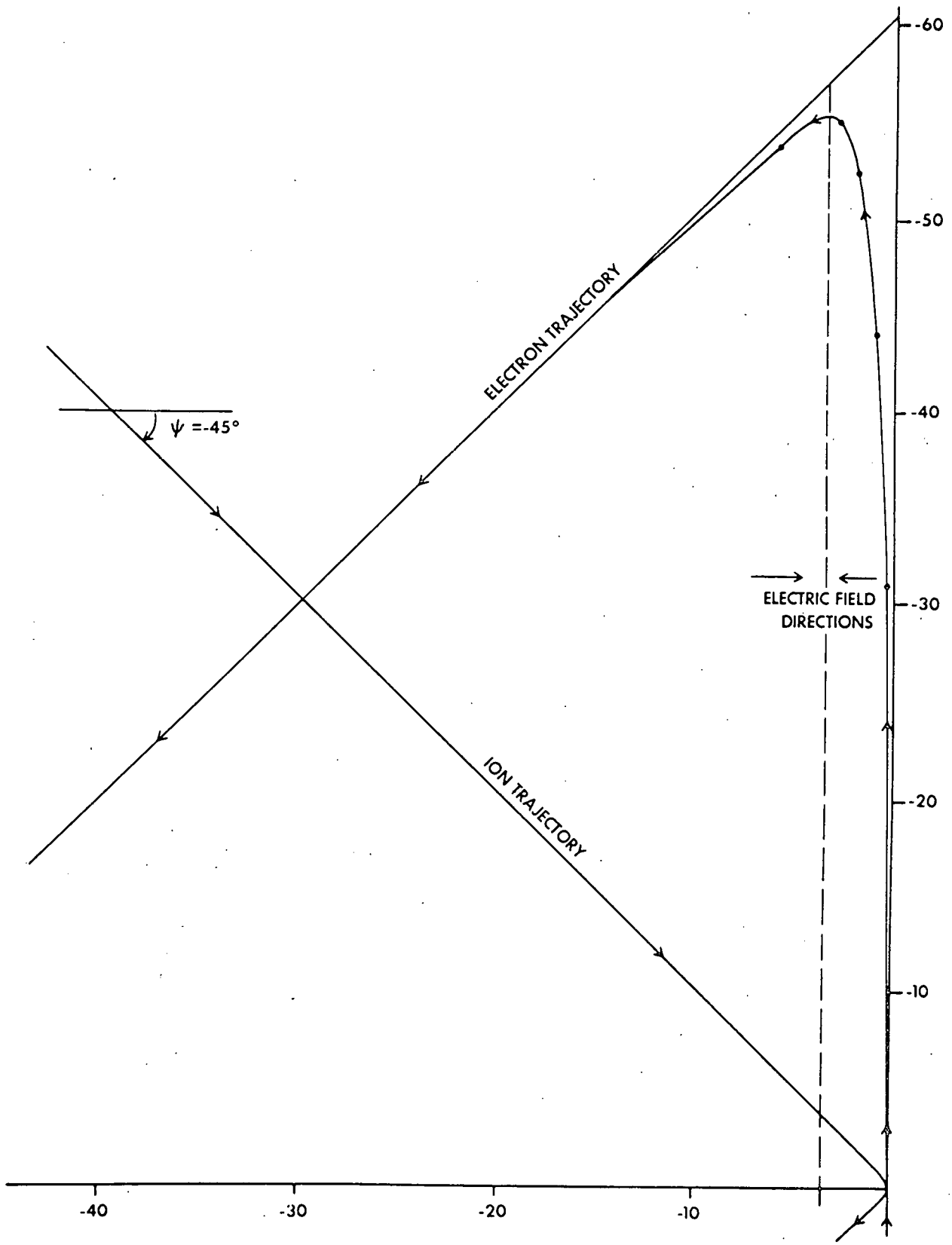
-60
-50
-40
-30
-20
-10
ELECTRON TRAJECTORY
ψ =-45°
ELECTRIC FIELD
DIRECTIONS
ION TRAJECTORY
-40
-30
-20
-10

Figure 2a

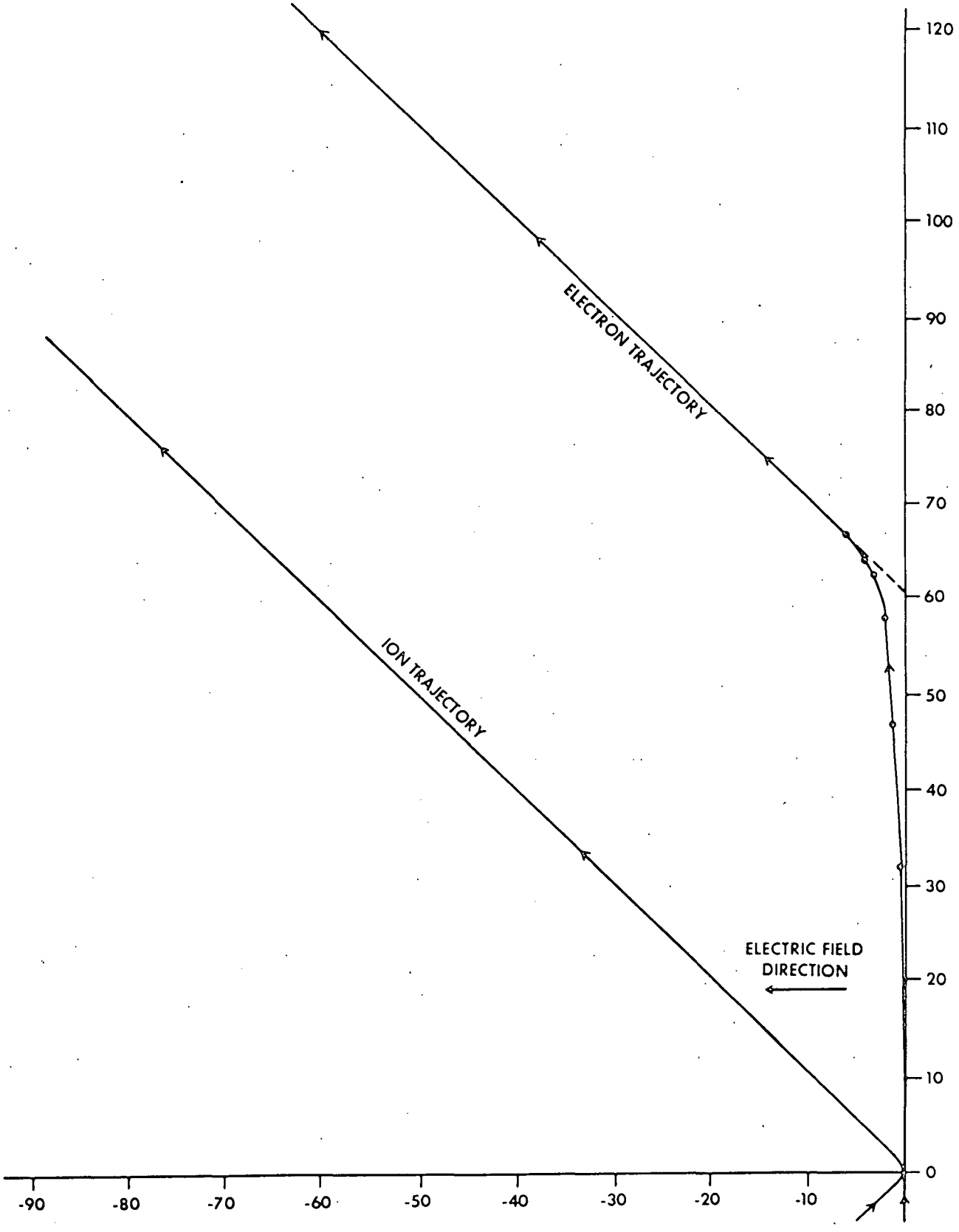
ELECTRON TRAJECTORY
ION TRAJECTORY
ELECTRIC FIELD
DIRECTION
120
110
100
90
80
70
60
50
40
30
20
10
0
-90
-80
-70
-60
-50
-40
-30
-20
-10

Figure 2b

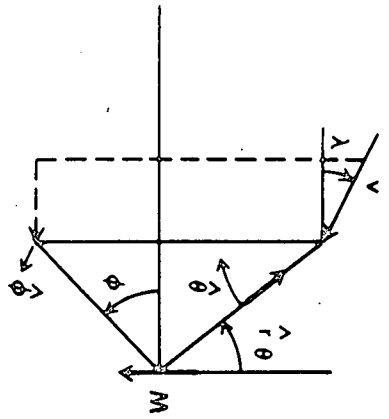

Figure 3

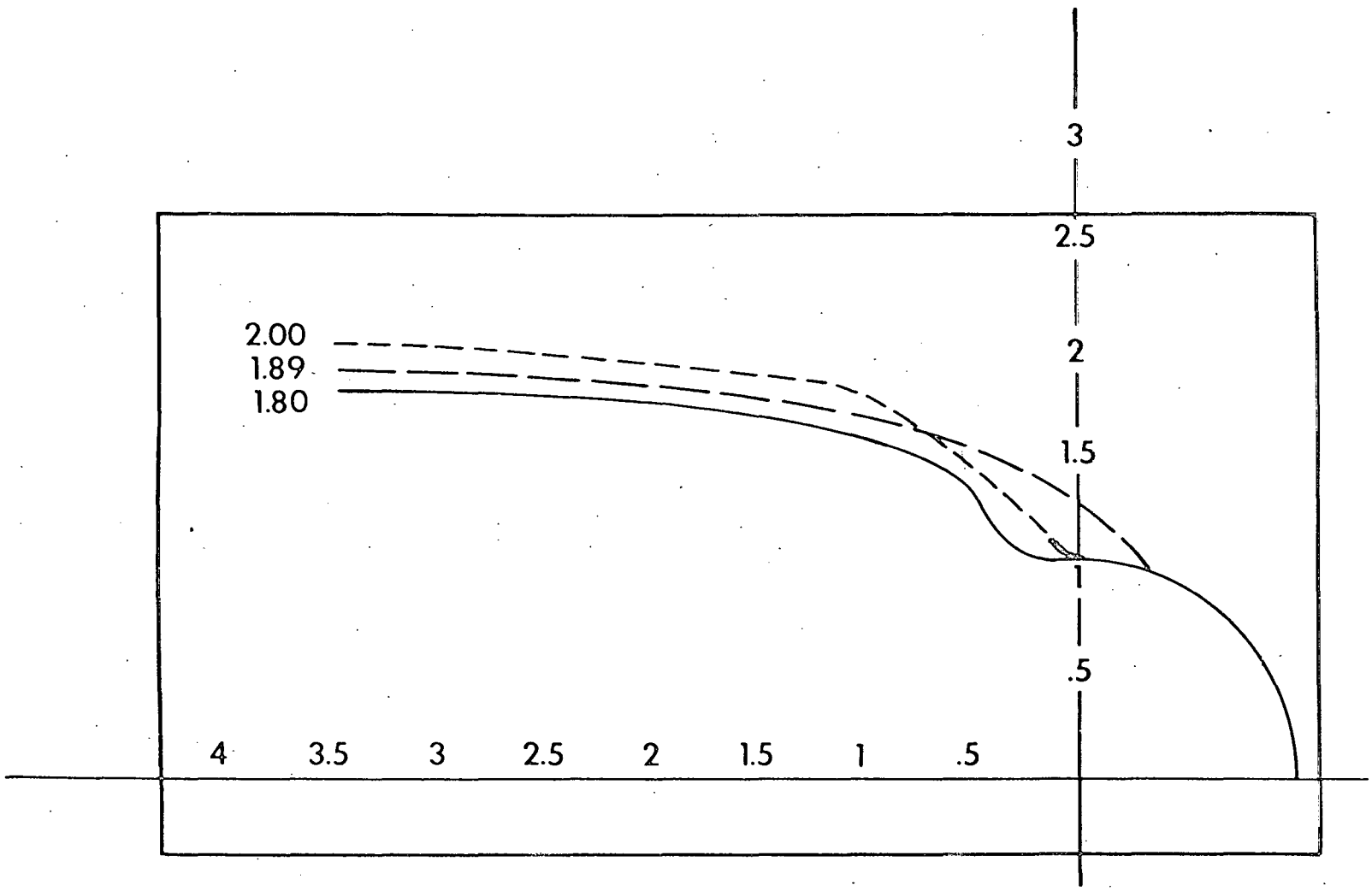

Figure 4

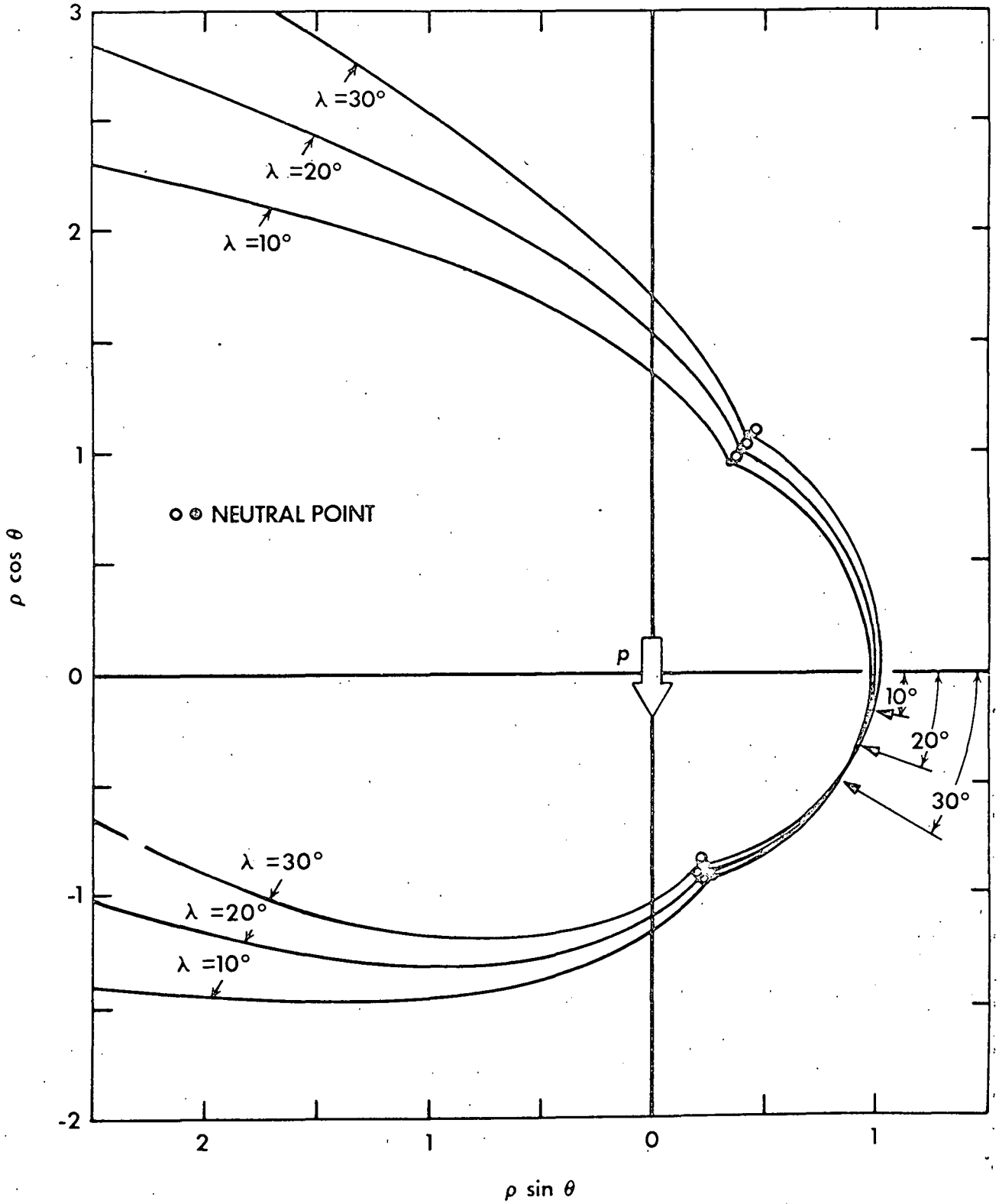
3
2
1
0
-1
-2
2
1
0
1
λ =30°
λ =20°
λ =10°
NEUTRAL POINT
p
10°
20°
30°
λ =30°
λ =20°
λ =10°
ρ cos θ
ρ sin θ

Figure 5

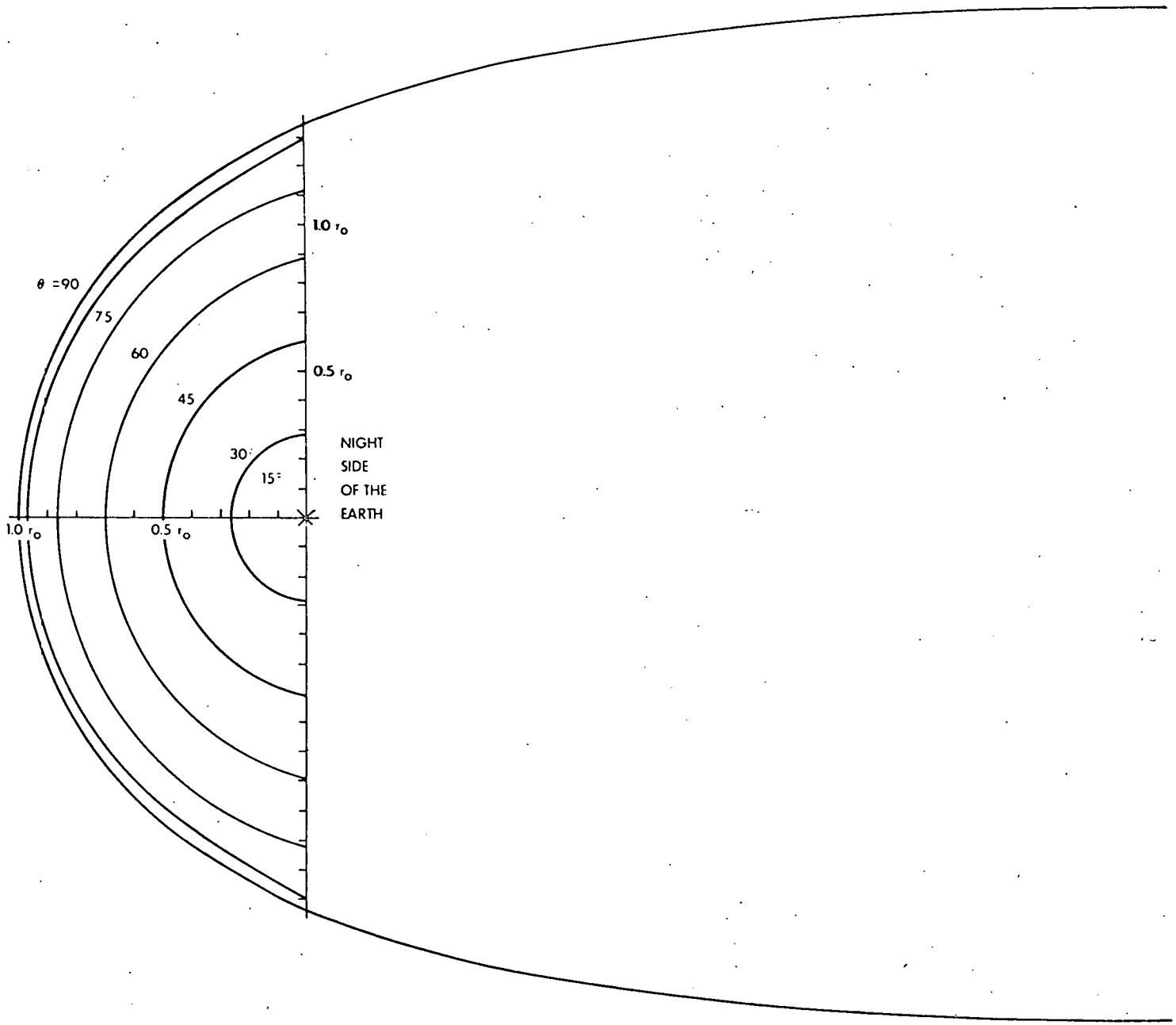
1.0 r_o
θ =90
75
60
45
30
15
0.5 r_o
NIGHT
SIDE
OF THE
EARTH
1.0 r_o
0.5 r_o

Figure 6

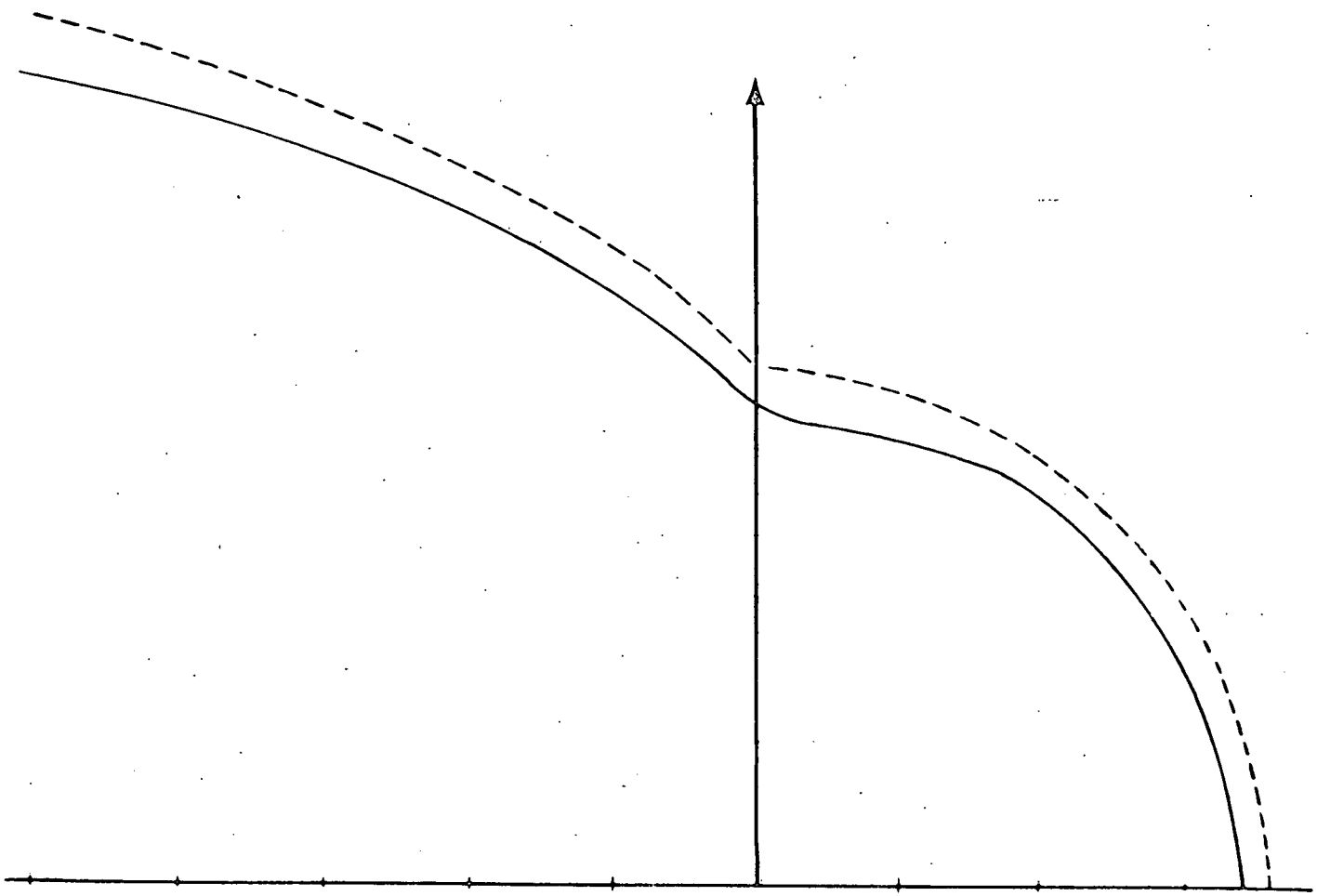

Figure 7

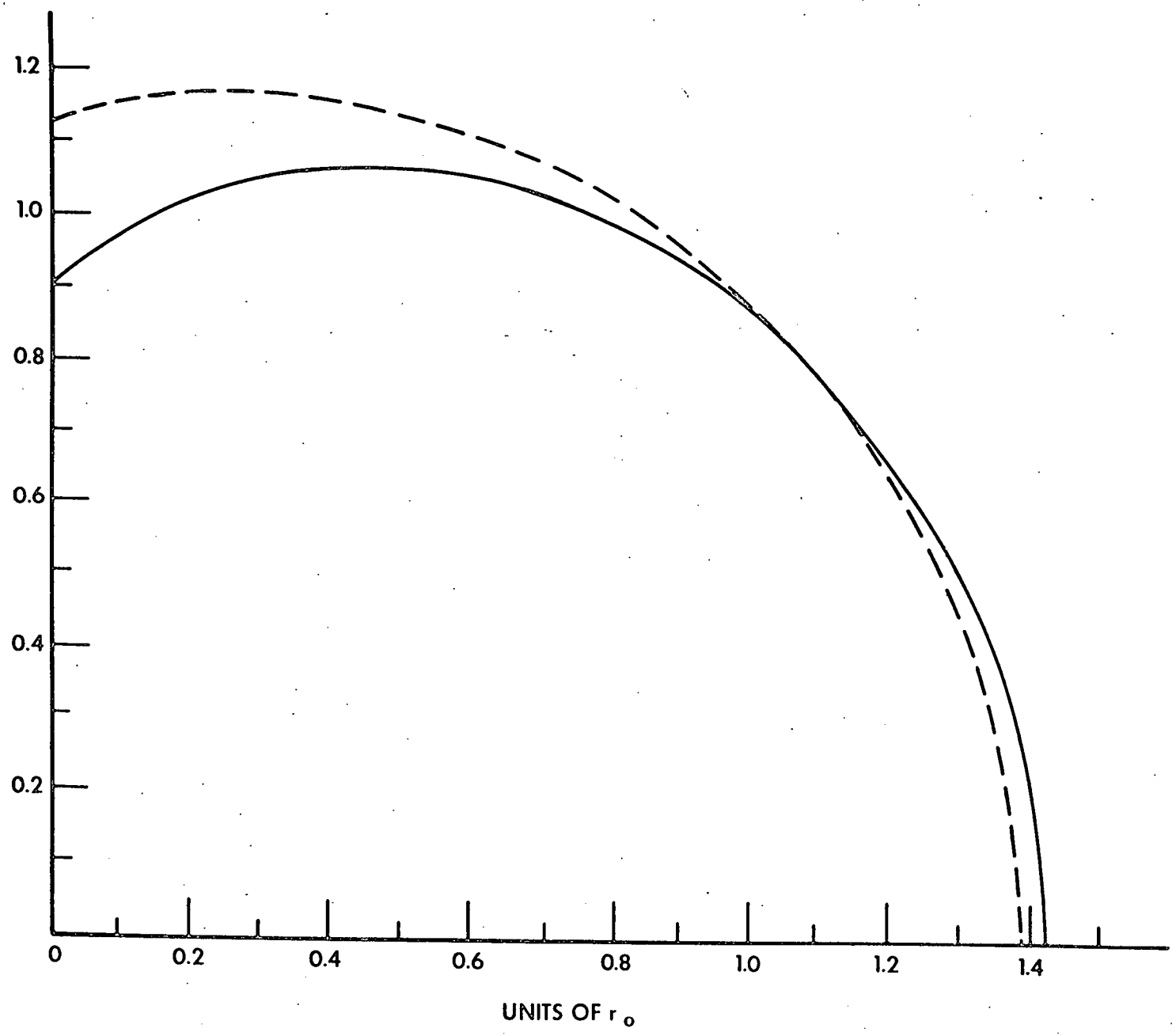

Figure 8

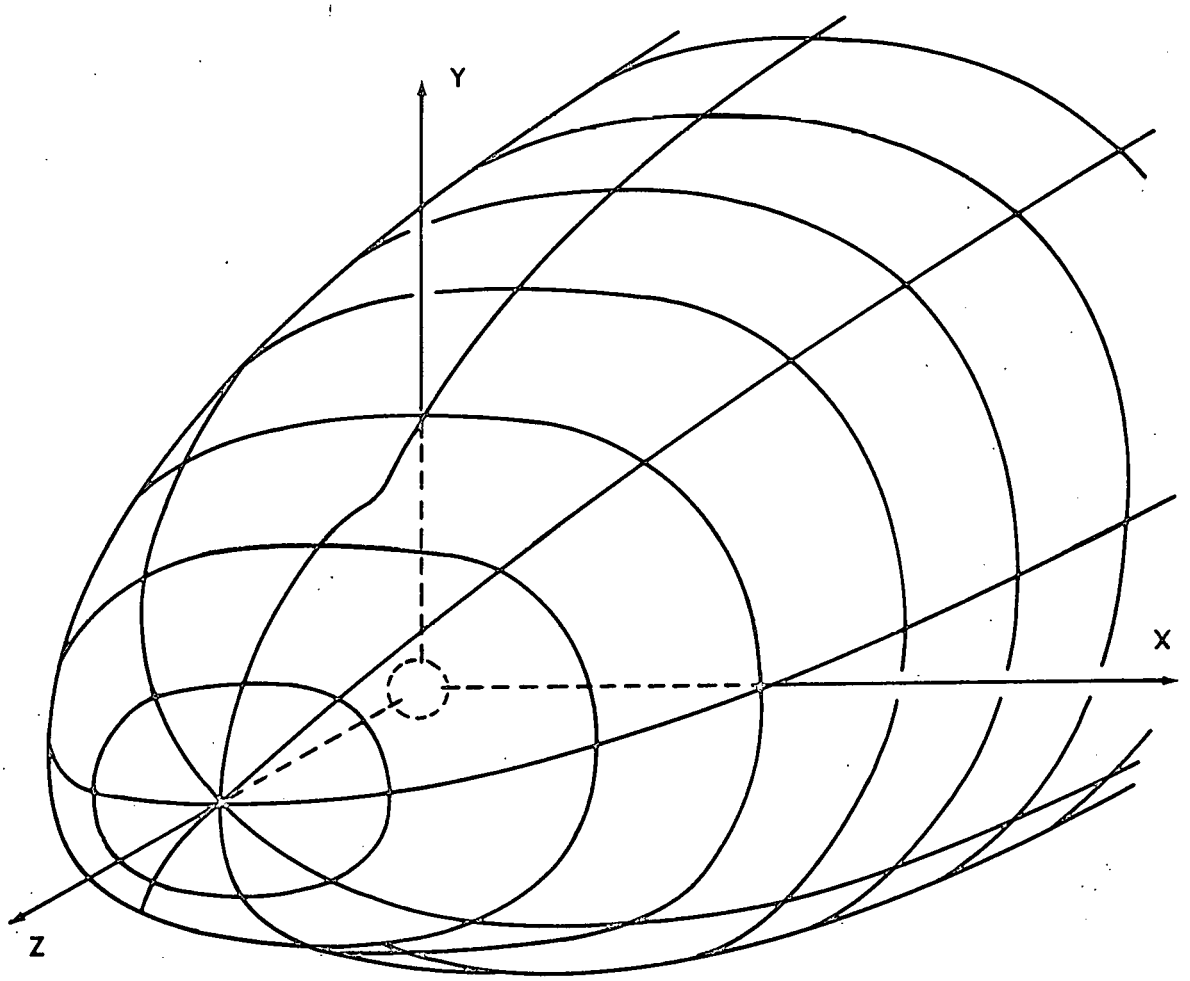

Figure 9

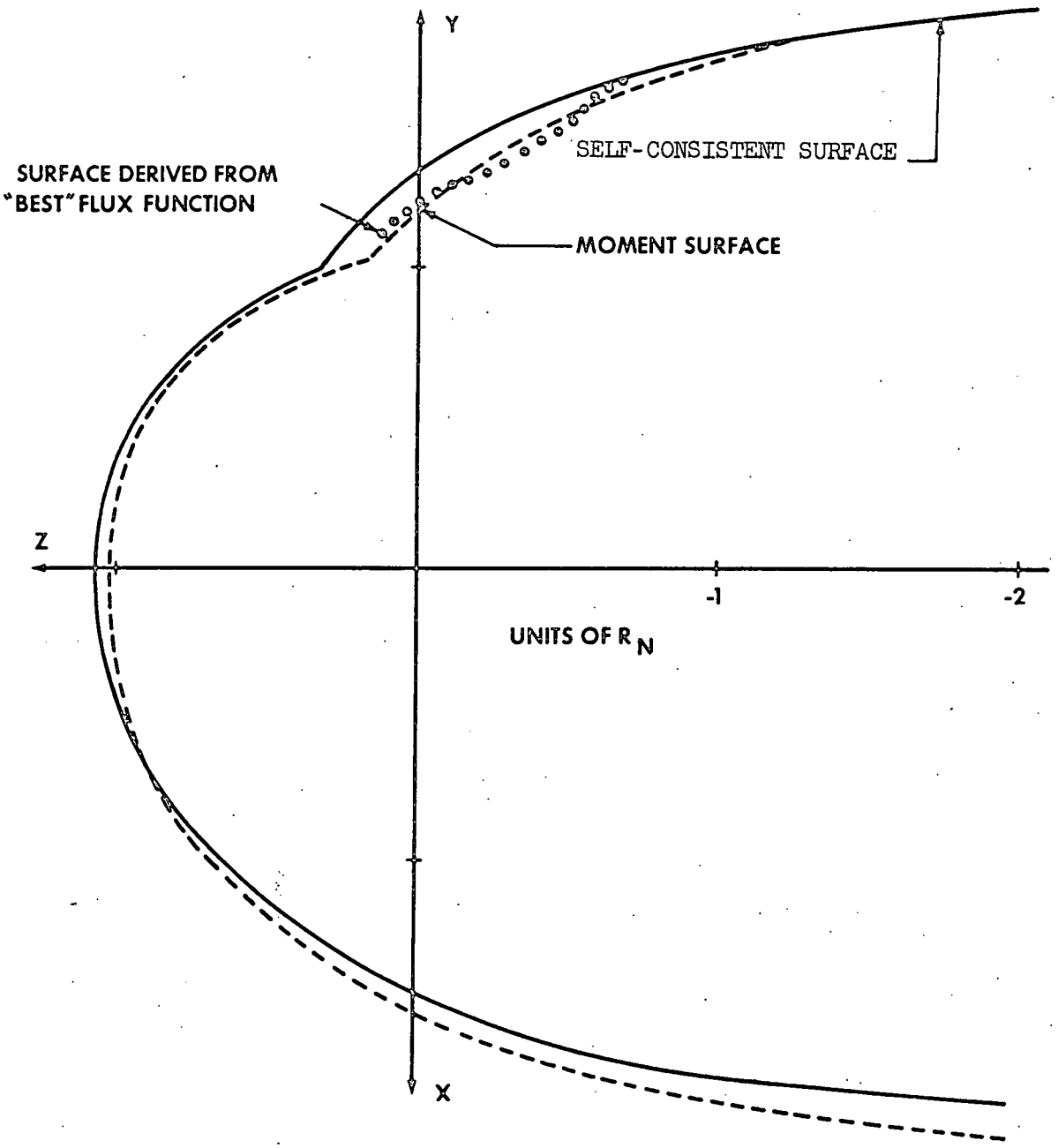
Y
SELF-CONSISTENT SURFACE
SURFACE DERIVED FROM
"BEST" FLUX FUNCTION
MOMENT SURFACE
Z
-1
-2
UNITS OF R_N
X

Figure 10

APPROXIMATE SURFACE FOR WIND/STATIC PRESSURE RATIO OF 10,000/1

(ESTIMATED ACCURACY IS SHOWN IN PERCENT OF RADIUS VECTOR)

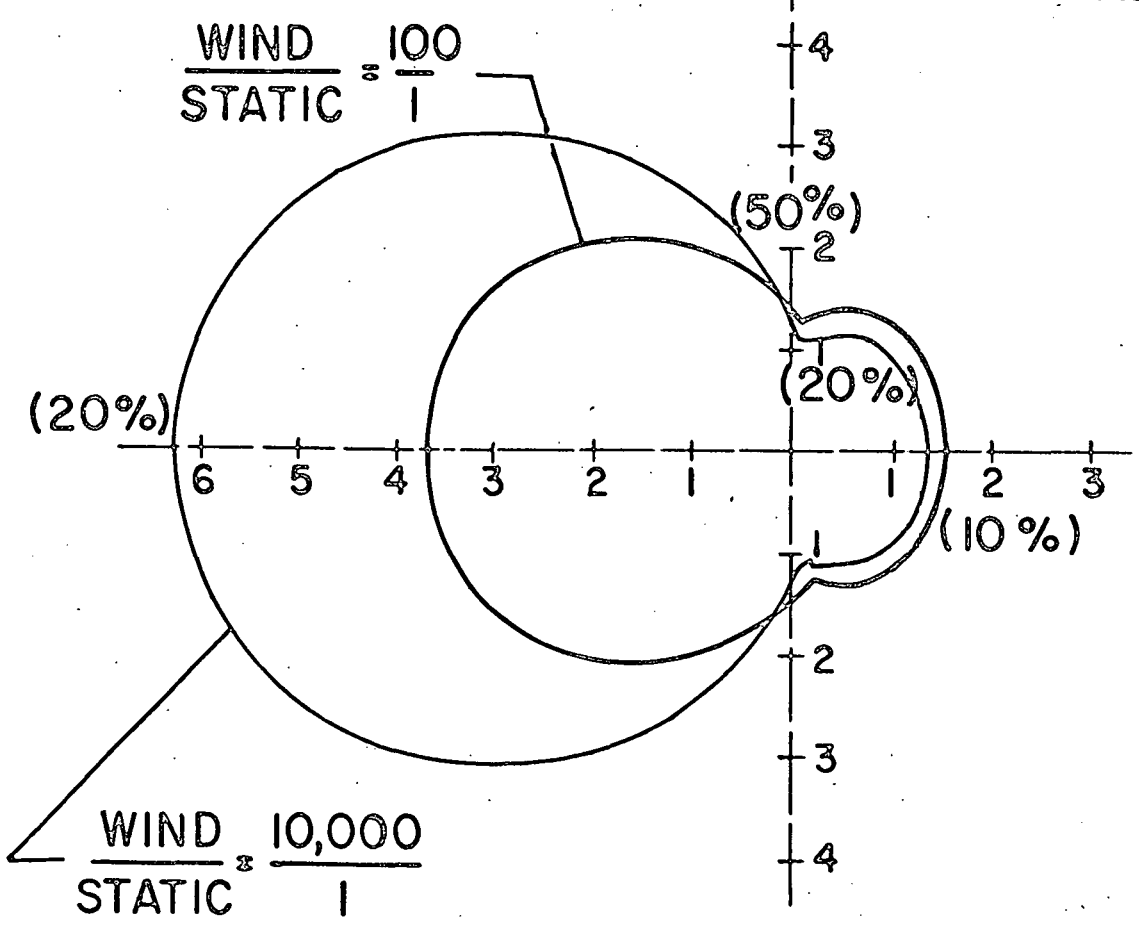

Figure 11

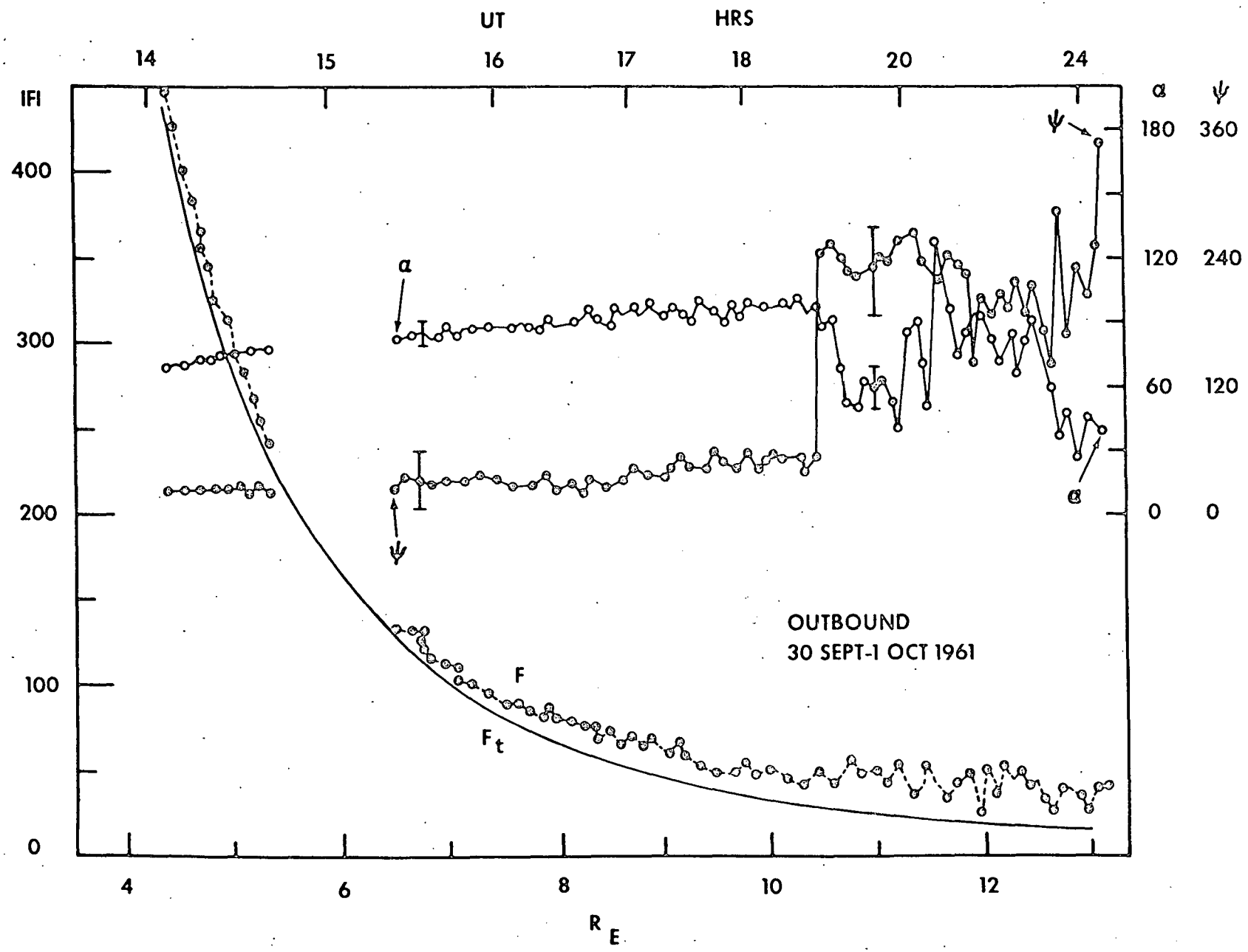
UT
HRS
14
15
16
17
18
20
24
IFI
400
300
200
100
0
α
ψ
180
360
120
240
60
120
0
0
α
ψ
OUTBOUND
30 SEPT-1 OCT 1961
F
F_t
4
6
8
10
12
R_E

Figure 12

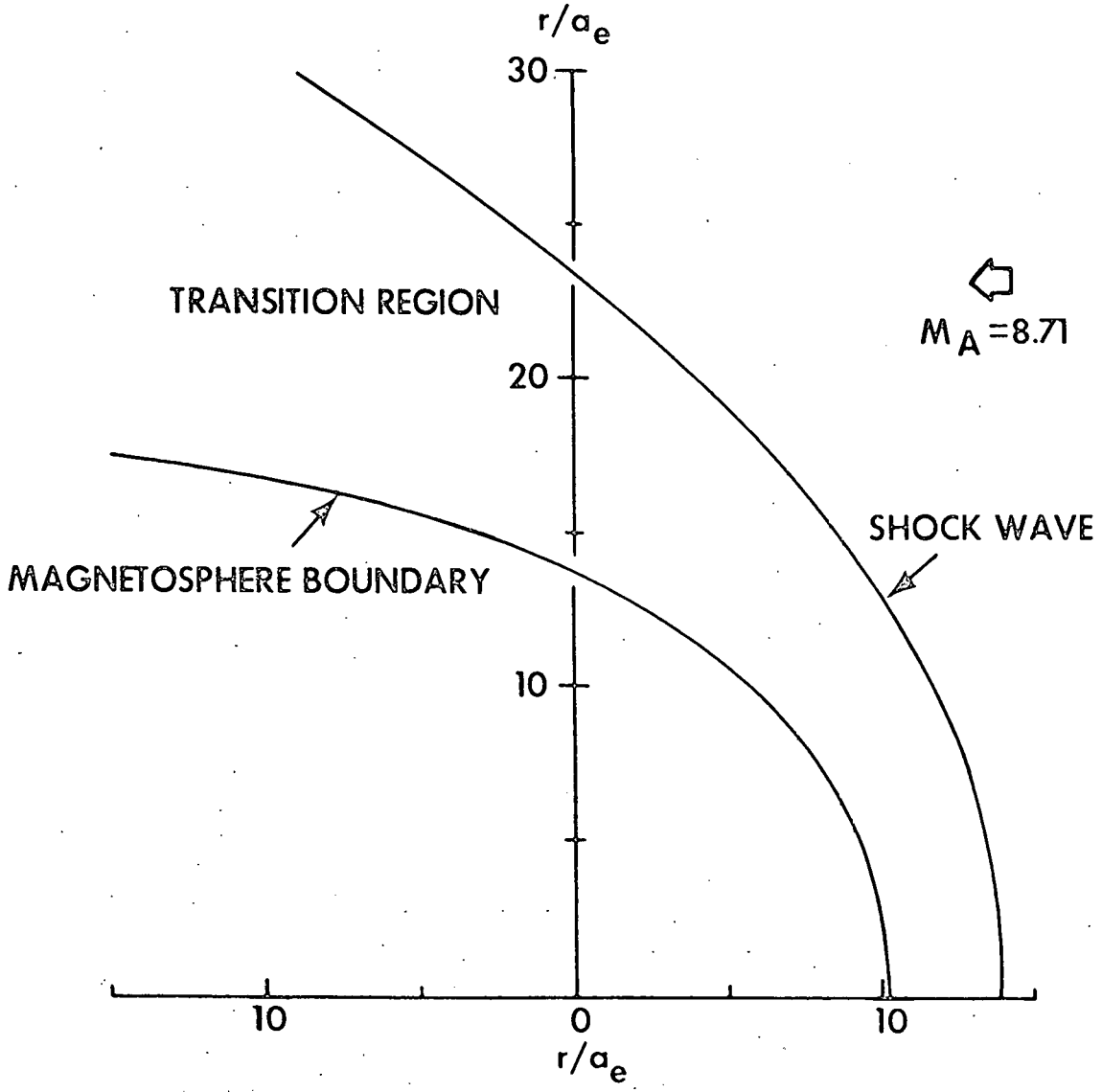
r/a_e
30
20
10
TRANSITION REGION
M_A=8.71
SHOCK WAVE
MAGNETOSPHERE BOUNDARY
10
0
10
r/a_e

Figure 13

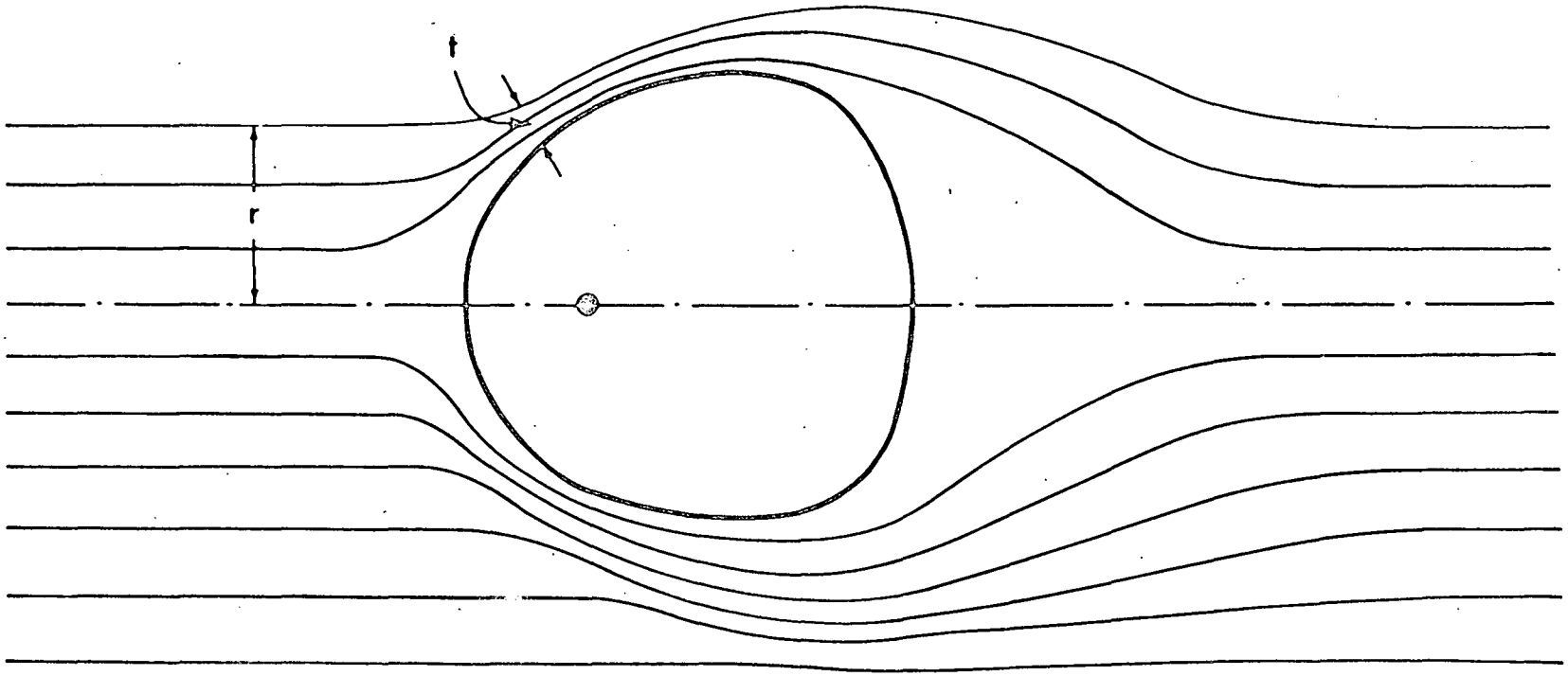

Figure 14